THE DAVID W. TAYLOR MODEL BASIN

UNITED STATES NAVY

TOEPLER'S SCHLIEREN METHOD

BASIC PRINCIPLES FOR ITS USE AND QUANTITATIVE EVALUATION

BY DR.-ING. HUBERT SCHARDIN, BERLIN

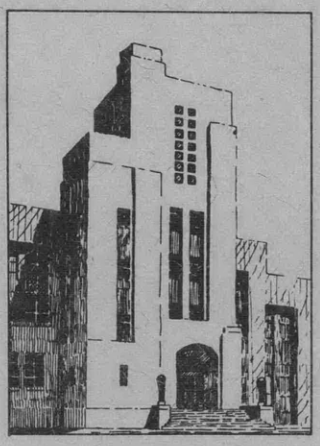

JULY 1947

TRANSLATION 156

TOEPLER'S SCHLIEREN METHOD
BASIC PRINCIPLES FOR ITS USE AND QUANTITATIVE EVALUATION

(DAS TOEPLERSCHE SCHLIERENVERFAHREN: GRUNDLAGEN
FÜR SEINE ANWENDUNG UND QUANTITATIVE AUSWERTUNG)

by

Dr.-Ing. Hubert Schardin, Berlin

FORSCHUNGSHEFT 367
Beilage zu "Forschung auf dem Gebiete des Ingenieurwesens"
Ausgabe B, Band 5, Juli/August 1934

Translated by F.A. Raven, Ph.D.

Navy Department
David Taylor Model Basin
Washington, D.C.

July 1947 Translation 156

NOTATION

a'	Distance from the edge of the image of the light source to the schlieren stop
$\Delta a'$	Variation of a' due to the light refraction in the schliere
B	Schlieren stop
C	Condenser
df	Element of surface
$d\omega$	Element of solid angle
E	Intensity of illumination
f, f'	Focal length
K	Schlieren objective
L	Light source
n	Index of refraction
O	Camera lens which projects the image of the schliere toward P
P	Ground glass or photographic plate
p	Pressure
R, r	Radii
S	Schliere
s	Distance from the schliere to the schlieren stop
T	Temperature
u	Angle of aperture
y	Distance from optical axis
$\mathfrak{B}$	Light density
β'	Lateral magnification
ϵ	Angle of deflection in the schliere
η	Coefficient
ρ	Density
Φ	Light flux

TABLE OF CONTENTS

TOEPLER'S SCHLIEREN METHOD
BASIC PRINCIPLES FOR ITS USE AND QUANTITATIVE EVALUATION

SUMMARY

The theoretical principles of Toepler's schlieren method are developed to a point which permits construction of the apparatus, suited to a definite purpose with the aid of the derived equations. It further permits calculating deflections of light within the object when the variations of density are known. Therefore, it can be predetermined whether application of the schlieren method promises success in a given case.

In simple cases the condition in the object is to be calculated inversely from the deflection of light. This eliminates the criticism that quantitative evaluation is impossible, which has always been a disadvantage of the schlieren method heretofore.

The most important fields of application are summarized, and the theoretical basis for each is treated, insofar as seems requisite for an exact application of the schlieren method.

INTRODUCTION

Toepler's schlieren method was described in the year 1864 by August Toepler. Four papers by him appeared in Poggendorff's Annalen which were later reprinted unchanged in "Ostwalds Klassiker der exakten Wissenschaften," Volumes 157 and 158, on the occasion of Toepler's seventieth birthday. Although the method has been used frequently, nothing hitherto published surpasses Toepler's original writings as far as basic principles are concerned. The present study will attempt to treat the individual parts of the schlieren arrangement successively and in greater detail, to permit recognition of the requirements for suitable construction and satisfactory application.

Concerning the pure shadow method, a study of E. Schmidt appeared in 1932, in which the quantitative evaluation of this method was described merely for a few simple cases. It is to be proved in the present paper that Toepler's schlieren method furnishes generally quantitative results. In conclusion, the most important fields of application will be treated.

The work was performed in the Institute of Technical Physics in the Technische Hochschule, Berlin. The author wishes to express his heartiest thanks to his respected teacher, Privy Councillor C. Cranz, for his continued encouragement and the support that he gave to the study. Further gratitude is expressed to Messrs. Pohl, Woehl, and Genning for aid in several experiments and calculations.

I. OPTICAL FUNDAMENTALS

1. PRINCIPLES OF TOEPLER'S SCHLIEREN METHOD

The principle of the method will be briefly presented by Figure 1. The symbol L represents a rectangular light source whose luminosity is constant over its entire surface. At one end M it is sharply cut off. The objective K, i.e., the schlieren objective, which is spherically and chromatically corrected to the highest degree, produces an image of the light source at L'. At the latter point there is a stop† B, whose knife edge is adjusted

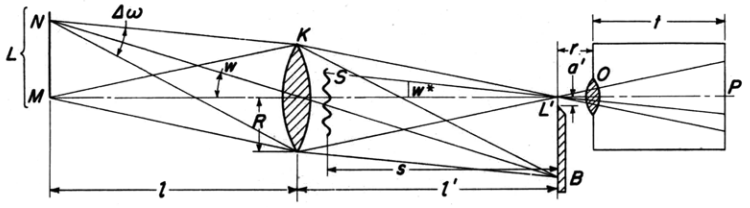

Figure 1 - Basic Arrangement of Toepler's Schlieren Method

L Light source; M and N, two points in it	O Camera lens which projects the schlieren image to P
L' Image of the light source	P Ground glass or photographic plate
K Schlieren objective	B Schlieren stop (knife edge)
	S Schliere

exactly parallel to the upper boundary of the image of the light source and which extends to within a distance a' from the edge of the image of the light source. The camera lens O produces a sharp image of the phenomenon S (schliere) to be investigated on the photographic plate or ground glass P. If the schliere had no deflecting effect on the light which traverses it, the optical field at P would necessarily be uniformly illuminated everywhere. However, if a deflection of the light occurs at a number of points on the schliere S, the images of these points must appear either brighter or darker depending upon whether the light which traverses the schliere is

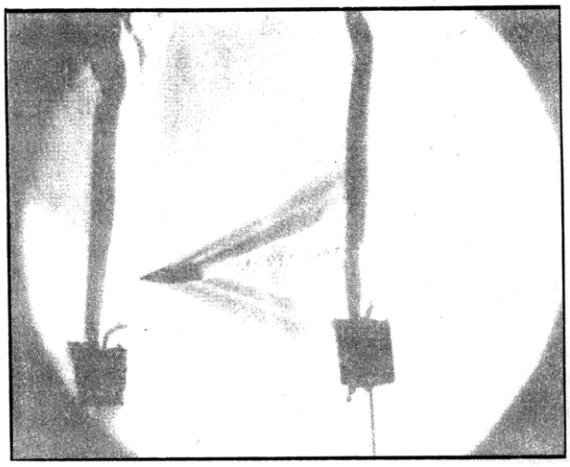

Figure 2 - Schlieren Photograph of a Projectile Traversing a Candle Flame

† Editor's Note: The author uses the word "Blende," equivalent to "diaphragm" in English, to designate this device, which may be a single knife edge, two knife edges, or four knife edges interposed between the schliere and the camera lens. In this translation, "Blende" and "Schlierenblende" are rendered as "stop" or "schlieren stop" unless a single knife edge is meant.

refracted more away from the edge of the schlieren stop or more toward it. Therefore, Toepler's schlieren method permits observation and measurement of very small light deflections such as are produced by nonuniformly heated air, for instance.

Figure 2, for example, shows the schlieren photograph of a burning candle. The heated air rising from the flame refracts the light on one side in a direction opposite to that on the other. Hence one side is brighter, the other darker, than the general background. This makes it appear as though the heated air were visible and illuminated laterally.

2. VARIATION OF BRIGHTNESS IN THE IMAGE AND THE ANGLE OF DEFLECTION IN THE SCHLIERE

First the intensity of illumination in the image of the light source will be calculated. The sharp edge of the light source should be located in the vicinity of the optical axis of the system. The light flux $d\Phi$, which comes from an element of area df lying in the optical axis and perpendicular to it and which falls into an element of the solid angle $d\omega$, is expressed by

$$d\Phi = \mathfrak{B}\, df \cos u\, d\omega \qquad [1]$$

with respect to the illuminated area according to Lambert's law. In Equation [1], $\mathfrak{B}$ denotes the flux density of the light source, and u denotes the angle formed by the element of solid angle and the optical axis. If $d\omega$ is a circular ring on a unit sphere described about df whose area equals $2\pi \sin u\, du$, Figure 3, then

$$d\Phi = \mathfrak{B}\, df \cos u\, 2\pi \sin u\, du \qquad [1a]$$

and integrating

$$\Phi = \mathfrak{B}\, \pi\, df \sin^2 u \qquad [2]$$

If the losses in the objective due to reflection and absorption are neglected, the same light flux is also present after refraction.†

$$\Phi = \Phi' = \pi\, \mathfrak{B}\, df \sin^2 u = \pi\, \mathfrak{B}'\, df' \sin^2 u' \qquad [3]$$

According to the sine condition which must be satisfied when reproducing a unit of area, the lateral enlargement β' is

$$\beta'^2 = \frac{df'}{df} = \frac{n^2 \sin^2 u}{n'^2 \sin^2 u'} \qquad [4]$$

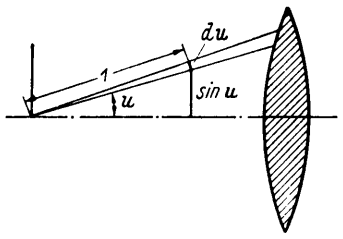

Figure 3 - Element of Solid Angle $d\omega$ Is the Circular Ring of Width du with $\sin u$ as Its Radius

† All values after refraction are indicated with the prime sign.

In the foregoing equation, n and n' signify the indexes of refraction in the object space and image space respectively.

From Equations [3] and [4] it is found that

$$\frac{\mathfrak{B}}{\mathfrak{B}'} = \frac{n^2}{n'^2} \qquad [5]$$

In the present case, $n = n'$; therefore, $\mathfrak{B} = \mathfrak{B}'$. The flux density in the image of the light source is hence equal to the flux density of the light source itself.

The intensity of illumination E' in the image of the light source in the vicinity of the axis is

$$E' = \eta \mathfrak{B} \pi \sin^2 u' \quad \text{or} \quad E' = \eta \frac{\mathfrak{B} \pi}{\beta'^2} \sin^2 u \qquad [6]$$

where the coefficient η accounts for the losses in the glass occasioned by reflection and absorption.

The brightness at the points in the image of the light source which are distant from the axis cannot be calculated in such a simple manner. According to Equation [1], the light flux emanating from an element df of surface on the light source which is distant from the optical axis and which enters the element of the solid angle $d\omega$ is

$$d\Phi = \mathfrak{B}\, df \cos w\, d\omega \qquad [7]$$

when the element of the solid angle is inclined by the angle w with respect to the normal to the surface, according to Figure 1. The same light flux traverses the image df' of df, with the exception of losses in the glass. Therefore, considering Equation [4]

$$d\Phi' = \mathfrak{B} \frac{df'}{\beta'^2} \cos w\, d\omega \qquad [8]$$

If the further assumption is now made that the angle w shown in Figure 1 is to be considered as the mean value of all w's, i.e., a small angle of aperture $\Delta\omega$, then

$$\Phi' = \frac{\mathfrak{B}\, df'}{\beta'^2} \cos w\, \Delta\omega \qquad [9]$$

Furthermore, if, as an approximation, we set

$$\Delta\omega = \pi R^2 \cos w : \left(\frac{l}{\cos w}\right)^2$$

where R denotes the radius of the schlieren objective and l signifies the distance from the light source to the objective, then

$$\Delta\omega = \frac{\pi R^2 \cos^3 w}{l^2} \qquad [10]$$

and with consideration for the losses of light

$$\Phi' = \eta \frac{\mathfrak{B}\, df'}{\beta'^2} \pi R^2 \frac{\cos^4 w}{l^2}$$

$$E' = \eta \frac{\mathfrak{B}}{\beta'^2} \pi R^2 \frac{\cos^4 w}{l^2} \qquad [12]$$

Equation [12] states that the brightness in the image of the light source decreases with the fourth power of the cosine ($\cos^4$) as the distance from the axis increases.

For example, when

w = 0 degree	$\cos^4 w$ = 1
1	0.99935
2	0.99760
3	0.99403
4	0.99028
5	0.98482

The light which passes the knife edge serves to locate the optical field on the ground glass P; see Figure 1. If the distance from the edge of the knife edge to the edge of the image of the light source is a', then, according to Equations [3] and [4], we set

$$\Phi' = \frac{\pi \mathfrak{B}}{\beta'^2} a' b' \sin^2 u \qquad [13]$$

where b' denotes the width of the image of the light source.

If the knife edge is shifted continuously in the vicinity of the optical axis, i.e., if the distance a' is changed continuously, the light flux which illuminates the optical field varies correspondingly. However, at a greater distance from the optical axis, the linearity would no longer be rigorously satisfied as a result of the decrease in the brilliance of the image of the light source at the rate of $\cos^4$. If it is desired not to exceed a margin of error of 1 per cent, the image angle, w in Figure 1, to which the light source is exploited, may only amount to 4 degrees in the maximum case.

An image of the schliere S is produced at P by the lens O in Figure 1. Every ray of light which traverses S is refracted in the lens O to the corresponding point of the image on the ground glass P. The angle at which the light emanates from the schliere is immaterial, presupposing, naturally, that it is not cut off by the knife edge or the frame of the objective. Therefore every element of the area df' in the image of the light source contributes to the brightness of the surface of every point in the image field at P. Consequently, according to Equation [13], the brightness of every point of the image field is exactly proportional linearly to the position of the knife edge within 1 per cent, as long as the image angle of the

effective light source with the axis does not exceed 4 degrees. The same variation in brightness as produced by shifting the knife edge by the value of $\Delta a'$ must naturally also be produced for a point in the image field, if the light rays undergo a deflection by the angle ϵ perpendicular to the knife edge as they traverse the corresponding point in the schliere. This deflection must be equally large for all rays traversing this point, and, moreover, equal to $\Delta a'/s$, where s is the distance from the schliere to the knife edge. The deflection of a light ray produced in the schliere naturally depends somewhat on the angle of incidence. Hence, the requirement that all rays undergo the same deflection is not satisfied. However, if a sufficiently small image angle of the light source is selected, the brightness at a point in the image field is very accurately proportional to the angle of deflection in the corresponding point on the schliere. It is naturally presumed in the foregoing that the light source itself produces constant brilliance over its surface and that the deflection is of such a type that

a. the constant field of illumination of the light source image will not be exceeded;

b. the deflected rays may still traverse the lens O;

c. the lateral extent of the light source will be sufficient; that is, that the total light source image will not be already completely broken down by the knife edge.

If the absolute value of the luminosity for all points in the image field is to depend linearly on the angle of deflection with the same factor of proportionality in the corresponding points of the schliere, the same luminosity must be everywhere present in the image field without schliere and at the same adjustment of the knife edge. If the flux density at the location of the schliere is designated by $\mathfrak{B}_s$, the intensity of illumination E^* in the image field corresponding to Equation [9] is

$$E^* = \frac{\mathfrak{B}_s}{\beta'^{*2}} \cos w^* \, \Delta\omega^* \qquad [14]$$

where w^*, $\Delta\omega^*$, and β'^* denote the same magnitudes as w, $\Delta\omega$, and β' in Equation [9], however, for the reproduction of a point within the schliere. Assuming that no artificial vignetting occurs, which will be reserved for later comment,

$$\Delta\omega^* = \frac{a' b' \cos w^*}{(s/\cos w^*)^2} \qquad [14a]$$

Furthermore, according to a theorem from the theory of ratios of luminosity in optical instruments, $\mathfrak{B}_s = \mathfrak{B}$; therefore .

$$E^* = \frac{\mathfrak{B}}{\beta'^{*2}} \frac{a'\,b'}{s^2} \cos^4 w^* \qquad [14b]$$

If the lateral magnification is set as $\beta'^* = \frac{t}{s+r}$, where r signified the distance between the knife edge and the front principal plane of the lens O,

$$E^* = \eta\,\mathfrak{B} \left(\frac{s+r}{t}\right)^2 \frac{a'\,b'}{s^2} \cos^4 w^* \qquad [15]$$

with consideration for the losses of light. The brightness in the image field also decreases toward the edge as the fourth power of the cosine ($\cos^4$). However, if an accuracy of 1 per cent is considered sufficient, the expression $\cos^4 w = 1$ can be written for values of w up to 4 degrees. Accordingly, within an angle of total aperture of 8 degrees, the intensity of illumination in the image field can be regarded as constant.

In Equation [15], moreover, r can be neglected with respect to s; therefore, by limiting cases to image angles below 8 degrees,

$$E^* = \eta \frac{\mathfrak{B}\,b'}{t^2}\,a' \qquad [16]$$

3. SENSITIVITY OF THE SCHLIEREN METHOD

It is here desired to answer the question as to which angles of deflection can just be made visible with the aid of Toepler's schlieren method. If the change in luminosity which can still be easily recognized is designated by $\alpha = \Delta E^*/E^*$, it can be calculated from Equation [16] how great the corresponding change $\Delta a' = \epsilon_m s$ is with respect to a', where ϵ_m denotes the smallest angle of deflection still visible. On the basis of the law of Weber-Fechner, this angle is to be expressed in ratio to E^*, for example

$$E^* + \Delta E^* = \eta \frac{\mathfrak{B}\,b'}{t^2}(a' + \Delta a') = \eta \frac{\mathfrak{B}\,b'}{t^2}(a' + \epsilon_m s)$$

Dividing by Equation [16],

$$\alpha = \frac{\epsilon_m s}{a'}; \quad \epsilon_m = \frac{a'}{s}\alpha \qquad [17]$$

The sensitivity of the schlieren method, therefore, depends on

a. the distance s, and

b. the extent to which the knife edge cuts off the image of the light source.

Theoretically, according to Equation [17] the sensitivity would have to become infinitely great for $a' = 0$, i.e., if the knife edge is screwed right

up to the edge of the image of the light source. Practically, however, natural limits are imposed on the sensitivity:

a. By the appearance of diffraction phenomena which become the more strongly noticeable the narrower the pencil of light rays becomes which is still admitted;

b. By the additional requirements that for a good recognition of the image of the schliere, there must also be a definite surface brightness of the image field.

According to Equation [16], a definite luminosity E^* could be maintained at every distance a', by varying the width b'. However, for technical reasons, an arbitrary increase of the width of the image of the light source is impossible.

Therefore, for a schlieren apparatus which employs a concave mirror with a focal length of 6.5 m (21.33 feet) and a diameter of 30 cm (11.81 inches) as a schlieren objective and a carbon arc lamp as a light source, the following sensitivity can be calculated. Let the flux density of the crater of the arc lamp B be about 15,000 *Stilbs*† (13,500 candles per square centimeter). For the intensity of the illumination in the image, 10 *Lux*†† = 10^{-3} *Phot*†† are required. If a 9-cm × 12-cm (3.54-inch × 4.72-inch) plate is to be illuminated, the distance t is found to be about 212 cm (83.46 inches). Let the maximum width b' of the image of the light source be 1 cm (0.394 inch), and the losses of light be 50 per cent. If these values are substituted into Equation [16],

$$10^{-3} = 0.5 \frac{15000 \cdot 1}{212^2} a', \text{ i.e., } a' = 6 \cdot 10^{-3} \text{ cm}$$

In the present case, s is approximately 500 cm (196.85 inches). Let the variation of brightness be set at about 5 per cent.‡ Therefore, the angle of deflection still visible is $\epsilon = 0.6 \times 10^{-6}$ radian = 0.124 second and $\Delta a' = 0.6 \times 10^{-6} \times 500$ cm = 3μ (microns).

---

† Translator's Note: The flux density of one *Stilb*, equivalent to the English lambert, is produced when 1 cm^2 of the luminous surface has a light intensity of 1 Hefner candle (HK). It is a unit of surface brightness equal to 0.9 International candles/cm^2 derived from Greek στιλβειν: to shine.

†† Translator's Note: A *Lux* is a lumen per square meter. A *Phot* is a lumen per square centimeter.

‡ α is a function of E^*; see König, Handbuch der Experimentalphysik, W. Wien and F. Harms, Vol.20, Leipzig, 1929, p. 65.

4. ARRANGEMENT OF THE SCHLIEREN STOP

The considerations which have just been established simultaneously furnish a working precept for focusing on schliere. Depending directly upon whether the object reveals strong or weak schliere, the distance a' must be increased or decreased by shifting the knife edge. Within certain limits, varying the width b permits adjustment to a definite surface brightness. Hence, from the same object at a larger value of a' and correspondingly smaller b', a weak image is obtained; whereas, if a' is decreased and b' is increased, the image becomes stronger. If the lateral extent of the image of the light source is small, then beyond a definite angle of deflection ϵ, the brightening in the corresponding points in the image field is no longer proportional to ϵ, but constant. This angle is determined from the deflection which is present if the entire image of the light source is intercepted by the knife edge. Likewise the linearity of the darkening of the optical field is only satisfied for deflections where $\epsilon < a'/s$. For greater angles, the entire light is intercepted by the knife edge. The corresponding points in the optical field must, therefore, be totally dark if no diffused light falls on the ground glass.

In the arrangement considered thus far, with a straight-edged schlieren stop which is introduced into the image of the light source from one side, only deflections perpendicular to the knife edge are visible. For deflections in other directions, only the component perpendicular to the knife edge is effective. Accordingly, the design of the schlieren stop will depend directly upon the type of object. Designs for the schlieren stop may be stated in which deflections in all directions are visible; for example, if the light source is circular and all direct light is precisely screened by a circular stop in the image of the light source. Under such conditions every deflection produced by a schliere must result in a brightening. It is possible also to admit all the direct light while intercepting all the irregular rays by a stop provided with a round aperture, in which case the schliere will appear dark upon a light background. It has been proposed frequently to screen off the image of the light source by both a horizontal and a vertical knife edge simultaneously. However, such an arrangement is exactly equivalent to a stop provided with a diagonal edge, for there must always be one direction in which the brightening due to refraction perpendicular to one knife edge is exactly equalized by the darkening resulting from the second knife edge. A deflection in this direction, therefore, is not visible.

In general, knowledge of the deflection in one direction suffices to give the conditions prevailing in the object; see Part II. Photography with a rectilinear knife edge is hence completely satisfactory. Moreover,

working with a curved stop would be entirely impossible when using concave mirrors for a schlieren objective as a consequence of the astigmatic image error. Furthermore, although the absolute value of the deflection at every point is known for a schlieren image when using a circular stop, the direction of the deflection is not known. Consequently, only schlieren stops with rectilinear edges and light sources with rectilinear boundaries will be here discussed.

The proper adjustment of the schlieren stop, which must be located at the image of the light source, can be undertaken as follows: First, by intercepting the image of the light source, an attempt is made to determine its approximate position. Then the schlieren stop is introduced from one side. The optical field on the ground glass P will first apparently be darkened from one side. Now, if this darkening occurs from the same side from which the knife edge was introduced, the stop must be removed farther from the ground glass. This corresponds to Position 1 in Figure 4. Conversely, darkening occurs if the sharp image of the light source is located between the schlieren stop and the ground glass, as in Position 2, Figure 4. Only when the stop is exactly at the image of the light source does the image field become uniformly dark. Any residual irregularities of brightness that may occur are to be traced to imperfections in the schlieren objective and the like. These will be treated in the next section.

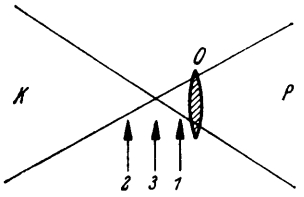

Figure 4 - Position 3 Is the Correct Location of the Schlieren Stop

Correct adjustment of the ground glass P may be explained at this point. When the schlieren stop is completely removed, all light rays which emanate from any given point on the schliere must attain corresponding points on the image. Therefore, a schliere must not be visible. However, if the ground glass is not located in the plane of the image, more pronounced schliere, such as those of a Bunsen flame, remain visible. The adjustment of the ground glass can, therefore, be undertaken by determining the place where nothing can be seen of the schliere without a schlieren stop. Thus a good mean adjustment can be made for photographing objects of greater depth.

5. QUALITY REQUIREMENTS OF THE SCHLIEREN OBJECTIVE WHEN USING LENSES

Since deflections of the light rays of the order of magnitude of 0.1 second produced by schliere cause a variation in brightness in the image field, it is requisite that the optical apparatus used as a schlieren

objective shall not reveal inherent irregularities within the above range in light refraction or of reflection for concave mirrors.

The glass itself must be free of flaws. For technical reasons, this requirement is especially hard to satisfy for large lenses. Figure 5 shows the streaks of an objective lens which had been fabricated for schlieren observations. If the flaws in the glass or the streaks in the cement are not too strong, the objective can still be used. Under such conditions it is known which streaks are to be ascribed to flaws in the lens in interpreting the phenomena.

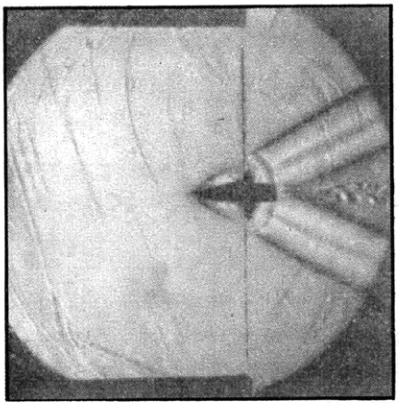

Figure 5 - Projectile Fired Through a Copper Strip

The optical field is filled with streaks resulting from the faulty structure of the schlieren objective.

The surfaces must be precisely ground and highly polished.

Spherical aberration must be eliminated to such an extent that the areas about the edge of the lens show the same brightness in the image field as does the center. This is not the case in an ordinary biconvex lens. As an example, the values for a crown-glass lens whose indexes of refraction are $n_D = 1.5096$, $n_F = 1.51525$, and $n_G = 1.59375$ will be given. The diameter and focal length will be selected to correspond to a concave mirror, with which most of the photographs were taken. If the radii of curvature $r_1 = -r_2 = 3057.6$ mm (120.38 inches), the thickness in the middle is 35 mm (1.38 inch), and the diameter of the lens $R = 300$ mm (11.81 inches), then the distance to the image $l' = +6000$ mm (+236.22 inches) for a distance to the objective of $l = -6000$ mm (-236.22 inches). If the schlieren stop is inserted at the image plane, the light rays traversing the edge of the lens are more sharply refracted; hence the edge acts like a fault which shifts the image of the light source on the stop by an amount $\Delta a'$ and thus produces a variation of brightness in the image field. The deflection $\Delta a'$ determined by optical calculation is shown in Figure 6. The plotted value $\Delta a'$ is valid for a variation of brightness of the image field in full scale, however, only for the diameter R of the lens which lies perpendicular to the

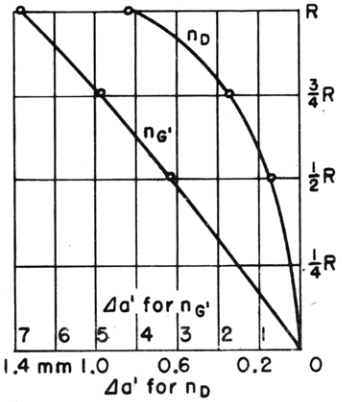

Figure 6 - Deflection $\Delta a'$ of Image of Light Source on Knife Edge with Biconvex Lens as Schlieren Objective

knife edge. A deflection of the light parallel to the edge does not cause any variation in brightness. Therefore, the effective deflection $\Delta a'$ for any arbitrary point on the lens is determined by reading the deflection with respect to the axis for the diameter concerned from Figure 6, and multiplying by the sine of the angle which the radius forms with the knife edge. In this way the curves of equal deflection, perpendicular to the edge of the stop, seen in Figure 7, were drawn. According to Equation [16], these curves are also curves of equal brightness in the schlieren image of the lens. Each successive curve signifies the same increase in brightness throughout, wherein it is assumed that the image of the light source is large enough not to be completely broken down by the schlieren stop for the points of great brightness, and that the distance a' between the edge of the screen and the edge of the image is sufficient to still permit light to enter for the darkest points. A photometric analysis of a schlieren image photograph would permit determination of the degree of correction of the lens.

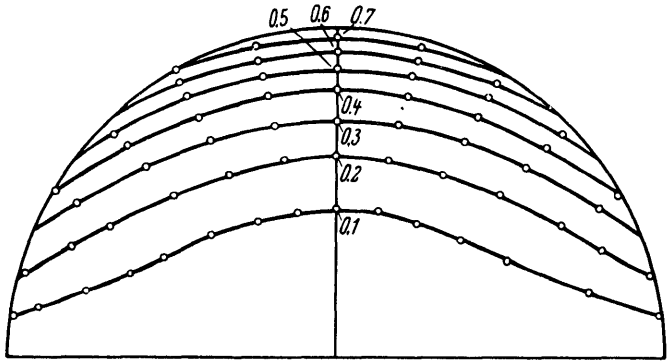

Figure 7 - Curves of Uniform Brightness in the Schlieren Image of a Biconvex Lens

It is apparent, therefore, that the spherical aberration of the lens can be investigated by means of the schlieren method. L. Foucault had already stated this; hence, Foucault's knife-edge test is to be regarded as the actual forerunner of Toepler's schlieren method.

According to the foregoing statements a simple biconvex lens is not suitable for a schlieren objective since no uniformly bright image field can be produced owing to the spherical error. This compels the use of an optical system which is corrected for spherical error.

When using a lens as a schlieren objective, the chromatic aberration must also be considered, for it will be all the more undesirable to use monochromatic light since this is impossible in many cases owing to considerations of brightness. The chromatic error of an objective becomes perceptible

because of varying distances of intersection of the light rays traversing the lens corresponding to the individual wave lengths of light. For the wave length whose light source image lies at the position of the schlieren stop, there would be uniform brightness on the ground glass, of course, but for all remaining ones there would not.

In Figure 8, the schlieren stop is located at the position of the image for the D-line. The image of the light source for the blue rays of the G'-line lies at G'. For these rays the upper edge of the lens deflects the image of the light source on the knife edge downward; the lower edge, in contrast, shifts it upward. Therefore, a blue image is superimposed on the uniformly bright yellow image on the ground glass. This blue image is brightest for the lower edge of the lens and darkest for the upper. If light from the spectrum line C is added, these rays produce an image of the light source at C. These evince a deflection with respect to the yellow rays opposite in direction from that of the blue ones. Hence an additional red image is superimposed on the image on the ground glass, which is brightest where the blue image is darkest. All in all, therefore, a very strongly chromatic image is produced upon the ground glass; the upper edge of the lens appears red, the lower blue; between these lie mixed colors. This may not be permitted for a satisfactory observation of schliere; hence the lens serving as a schlieren objective must be corrected chromatically.

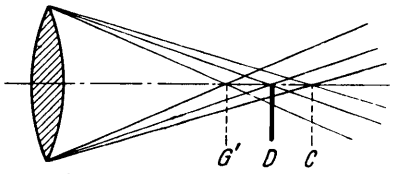

Figure 8 - Effect of a Chromatic Error of Schlieren Objective on the Schlieren Image

Astigmatic image defects, coma, and distortion, on the other hand, are negligible since the size of the light source reproduced by the schlieren objective is so small that the errors mentioned remain sufficiently small without correction, provided only that the sine condition is satisfied sufficiently.

Summarizing, it can be said with respect to the suitability of objectives that only those which have been corrected both spherically and chromatically to the best possible extent can be used for schlieren objectives. The glass of the lenses should be free of streaks and bubbles because all local defects are visible in the optical field. Furthermore, for the investigation of extended phenomena, lenses of maximum possible diameter are desirable. To obtain high sensitivity, long focal length must be selected according to Equation [17]. The fabrication of such lenses is not simple;

the expense is considerable. Telescope objective lenses of long focal length, as used for astronomical purposes, are best suited. Their condition of correction would be best utilized by arranging two identical objectives to

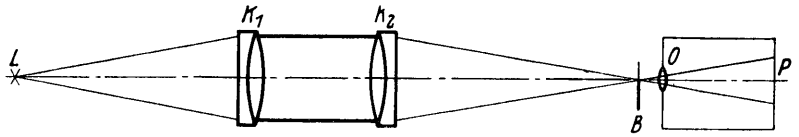

Figure 9 - Use of Two Astronomical Telescope Objective Lenses, K_1 and K_2, as a Schlieren Objective

produce a parallel beam between them; see Figure 9. In such a case the objectives can simultaneously perform the function of seals for the space in which the phenomena of flow in a gas occur which are to be investigated.

6. QUALITY REQUIREMENTS OF THE SCHLIEREN OBJECTIVE WHEN USING CONCAVE MIRRORS

It is desirable to use a concave mirror, silvered on its concave surface, as a schlieren objective instead of a biconvex lens, for the former is free of chromatic error. Moreover, streaks or flaws within the glass have no effect on the optical quality. Finally, mirrors can be fabricated with much greater diameter than lenses. For the same reason reflectors are generally used in astronomy instead of refractors. There are various possible applications of a concave mirror for present purposes.

Figure 10, for example, shows one arrangement which, however, includes the immediate disadvantage that the light source disturbs uniform illumination of the image field. In conjunction with the sharp image of the schliere S, a blurred image of the light source appears on the plate. Moreover, investigations must be made to determine whether the spherical errors are sufficiently small. The calculation using the values: distance $\overline{LB}$ 6 m (19.68 feet), distance $\overline{KL}$ 1 m (3.28 feet) gives the same order of magnitude for the spherical errors as the previously calculated biconvex lens, i.e., such an arrangement is not suited practically for a sensitive revelation of schliere.

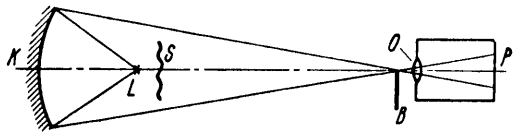

Figure 10 - A Possible Arrangement for the Use of a Concave Mirror as a Schlieren Objective

This arrangement is not very satisfactory.

In a concave mirror, reproduction from center of curvature to center of curvature takes place without error. Therefore it will be attempted so to modify the arrangement just described, which produces excessive spherical errors, that the image becomes almost aplanatic. A possible method is the so-called coincidence method which was probably first applied by H. Boas and was recently applied anew by Taylor and Waldram; see Figure 11.

A mirror placed obliquely at the center of curvature of the concave mirror serves as a schlieren stop and light source simultaneously. Its effect as a light source is based on the fact that from a suitable direction the light source L* is projected on the front surface of the plane mirror or prism through a condensing lens C. The advantage of this method consists in the fact that the concave mirror is thus used to the best advantage optically. However, a disadvantage is that the light rays traverse the schliere twice. A deflection occurs the first time that a light ray traverses the schliere. Then, after being reflected from the concave mirror, this ray impinges at another point on the schliere. The angle of deflection of the light rays is no longer only a function of the requisite location on the schliere. Consequently the schlieren image obtained is difficult to interpret. However, the smaller the deflection in the schliere, the less important this objection becomes. Thus the method is very suitable if only very small deflections are produced by the schliere. This follows because for small angles of deflection the total deflection of the rays impinging on the schlieren stop becomes approximately 2ϵ as a result of the double traversal of each light ray at approximately the same point on the schliere. Therefore, this method is about twice as sensitive as other methods.

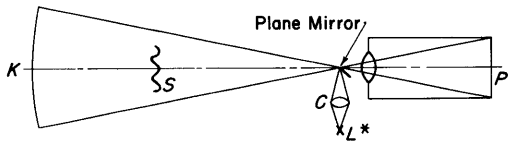

Figure 11 - Coincidence Method

The appearance of double images of objects located at the position of the schliere is avoided if the camera lens is brought as close as possible to the center of curvature; for, seen from the center point, the objects coincide with their reflected images.

To make very weak schliere visible the light may be sent repeatedly through the schliere, instead of only twice. A possible realization of this concept is shown in Figures 12 and 13. The light from the light source L*, in Figure 12, impinges on the concave mirror K_1 through the prism Q_1. This concave mirror projects an image of the light source slit at b; see Figure 13. The light now goes to the concave mirror K_2 whose axis does not exactly coincide with that of K_1; this produces an additional image of the light

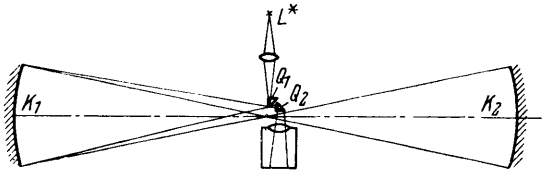

Figure 12

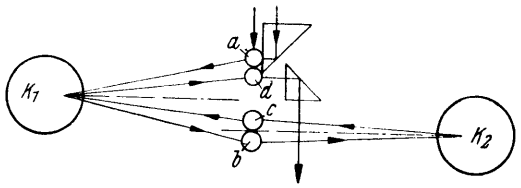

Figure 13

Figures 12 and 13 - An Arrangement to Permit Light to Repeatedly Traverse the Schliere in Order to Attain High Sensitivity

source at c. Now the schliere is once more traversed by the rays, the image d falls upon the prism Q_1 in exactly such a way that the edge of Q_1 functions as a schlieren stop. Then the light finally enters the photographic camera through the prism Q_2.

In this arrangement the schliere is traversed four times by the rays. Therefore the sensitivity should be about four times as great as when the light traverses it only once. A few experiments were made according to this method. However, it was found that the space available for the tests was not sufficiently shockproof to permit satisfactory testing of the arrangement. Moreover, its adjustment itself is very delicate. Nevertheless, the sensitivity in fact seemed to be considerably increased.

At rather large deflections the coincidence method is not usable. An arrangement must be found where the light traverses the schliere but once, and moreover, the light source and its image must lie as near as possible to the center of curvature of the concave mirror to prevent the disturbing effect of spherical error. Furthermore, the distance from the schliere to the schlieren stop must be so great that sufficient sensitivity is still available. These requirements can be satisfied by an arrangement wherein the light source L is located to the side of the center of curvature M; see Figure 14. The light cones impinging upon and reflected by the concave mirror intersect in one range. As the schliere cannot be located in this range, it cannot be moved arbitrarily near the concave mirror. If the schliere is to be 1000 mm (39.37 inches) distant from the concave mirror with a radius of curvature of 6000 mm (236.22 inches) and a diameter of 300 mm (11.81 inches), the distance from the light source to the midpoint M of the concave mirror must be

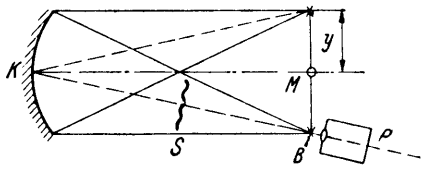

Figure 14 - Most Satisfactory Arrangement when Using a Concave Mirror as a Schlieren Objective

$$y = \frac{5000 \times 150}{1000} = 750 \text{ mm } (29.53 \text{ inches}).$$

The image of the light source in the present case is produced by an oblique pencil of rays. Hence astigmatic image errors occur. Even for rays which are near the axis all the light rays emanating from a point on the light source no longer converge at one point. Rather, there are different image points for tangential rays, i.e., rays lying in the horizontal plane, and for the sagittal rays, i.e., those in the vertical plane; for the example selected previously, this astigmatic difference is plotted in Figure 15. It is, however, relatively unimportant with respect to Toepler's schlieren method, for the latter method is not concerned with a deflection parallel to the edge of the schlieren stop. Accordingly, the stop must be located either in the sagittal or the tangential image point of the light source. Furthermore, it is essential that the rectilinear edge of the light source be exactly in or perpendicular to the plane which is defined by three points, light source, center of the mirror, and the image of the light source. Otherwise no sharply delineated edge of the light source is produced. However, the knife edge must also satisfy this condition and run exactly parallel to the edge of the light source. If this is not the case, uniform brightness in the image field cannot be obtained when screening off, for, as a result of the astigmatic error in the reproduction of the light source, both sides of the light beam which is still admitted by the schlieren stop do not contribute equally to the illumination of all points on the optical field; see Figure 16. Therefore if the schlieren stop which is

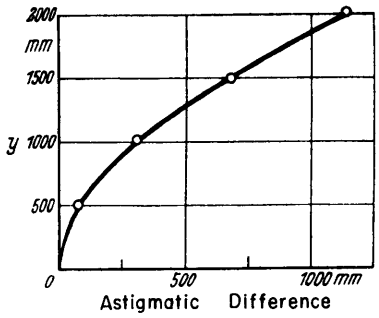

Figure 15 - Astigmatic Image Difference when Using a Concave Mirror

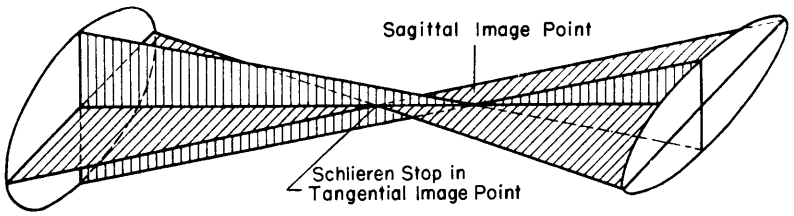

Figure 16 - Tangential and Sagittal Image Point when Projecting with a Concave Mirror

effective in the tangential image point has a component in that direction as it would have to for the sagittal image point, this component affects the brightness in the image field in the same way as if there were no schlieren

stop present in the image plane of the light source; compare Part I, Section 4. Therefore it is customary in practice first to shift the stop back and forth to find the place where one-sided darkening of the field of view no longer occurs in the direction of screening. Then the stop must be rotated until the brightness is distributed with complete uniformity in the perpendicular direction also.

It follows from the foregoing that the edges of the schlieren stop must be precisely rectilinear. An edge with a serrated appearance under a microscope would produce an optical field traversed by light and dark bands.

In addition, the effect of the spherical image error must be considered. For example, consider once more a mirror whose radius of curvature is 6000 mm (236.22 inches) and whose diameter is 300 mm (11.81 inches). The light source should be 500 mm (19.68 inches) to the side of the center of curvature. Previously 750 mm (29.53 inches) were calculated as the approximate minimum value. Let the difference between the sagittal and the tangential image points of the light source be 82.456 mm (3.246 inches). Let the schlieren stop with knife edge vertical now be inserted at the tangential image point; see Figure 16. Then the rays from the upper and lower edges impinge upon the knife edge at a distance from the tangential image point indicated in Figure 17. From the values indicated, a deflection on the knife edge of 6μ results for the ray from the upper edge and a deflection of 5μ for that from the lower. In Section 3, a deflection of 3μ on the stop was calculated as the approximate limit of sensitivity of the schlieren method.

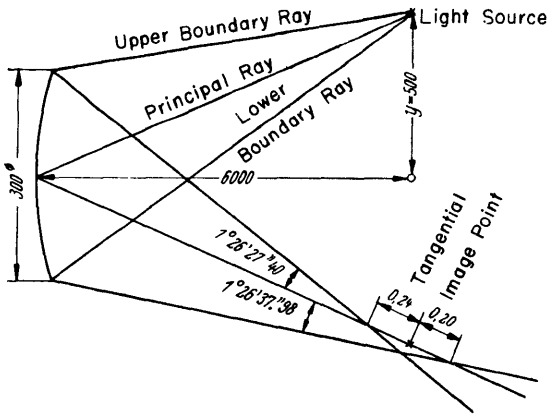

Figure 17 - Spherical Image Error in Projecting by a Concave Mirror

Therefore, it can be stated conclusively that the exactitude of reproduction of the light source via a concave mirror, corresponding to the arrangement in Figure 16, suffices to attain the approximate limit of sensitivity of the schlieren method. The effect of diffraction is treated in Part IV.

In the investigation of phenomena requiring parallel light, the arrangement just described cannot be used. Instead, a design corresponding to Figure 18 provided with two concave mirrors must be used. It might be believed at first that this arrangement would permit attainment of a very high sensitivity since the distance between the schliere and the mirror K_2

can be made arbitrarily great. However, this is not the case. If the distance from the schliere to the concave mirror K_2 is designated by s_k, then the image of the schliere produced by K_2 is $s'_k = \frac{s_k f}{s_k - f}$ distant from K_2, where f represents the focal length of the concave mirror.

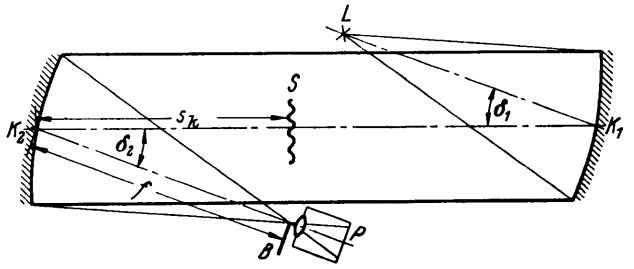

Figure 18 - To Get a Light Beam Composed of Parallel Rays, Two Concave Mirrors Must Be Used

If the schliere deflects a light ray by the angle ϵ, this signifies a deflection of the ray on the concave mirror whose magnitude is ϵs_k. The deflection $\Delta a'$ thereby produced on the knife edge is

$$\Delta a' = \frac{\varepsilon s_k (s'_k - f)}{s'_k} = \frac{\varepsilon s_k \left(\frac{s_k f}{s_k - f} - f\right)}{\frac{s_k f}{s_k - f}} = \varepsilon f \qquad [18]$$

Hence the sensitivity is not a function of the position of the schliere in the parallel beam of rays; it is as large as if the schliere were $f = r/2$ removed from the knife edge. Therefore the sensitivity is smaller than according to the preceding arrangement described. Since the sensitivity of the arrangement is independent of the position of the schliere between K_1 and K_2, the mirror can simultaneously be used to reproduce the schliere. In this way the lens O can be eliminated, and therefore the size of the deflection is not limited by the aperture of the foregoing lens. However, under such conditions, an astigmatic error in the reproduction of the schliere must be accepted. Moreover, in this arrangement, the question must be answered whether it is more favorable to place the light source and the knife edge on the same side or opposite sides of the line connecting the midpoints of the mirrors with respect to the spherical aberration in the oblique pencil, i.e., coma, and whether it is advantageous to make the two angles of avertance δ_1 and δ_2 of different size; see Figure 18. These problems were investigated basically in the Institute for Technical Optics of the Technische Hochschule Berlin by Professors Weibert and Ströble. It was found that the asymmetry in the tangential section is eliminated if the light source and the knife edge lie on opposite sides of the line connecting the center points of the mirrors, and moreover, if the angles of avertance are made equally large for mirrors of equal focal lengths. Professor Czerny achieved the same results experimentally.

7. ARRANGEMENT OF THE LIGHT SOURCE

In the considerations up to this point, it was assumed that a uniformly radiating illuminated surface was available which was sharply severed at one end. Only in the fewest cases will it suffice to use the actual light source itself, such as an arc lamp, spark gap, or sodium-vapor lamp. It will be preferable to produce first an intermediate image of the light source. This image can be limited arbitrarily by a stop. Moreover, the illuminated area can be projected enlarged. The aperture of the illuminating system $u_{c'}$ must naturally be at least the same as that of the schlieren arrangement u; according to Figure 19,

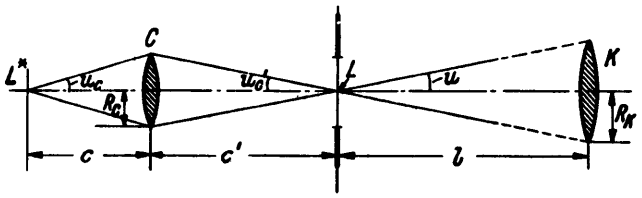

Figure 19 - The Illuminating System and the Schlieren Arrangement Have the Same Aperture

Here $u_{c'} = u$, L* is the light source, and L is the intermediate image of the light source.

$$R_c : c' = R_K : l$$

Furthermore, if the aperture ratio of the condenser is designated by v and the focal length by f_c, then

$$2R_c : f_c = 1 : v$$

and

$$c' = \frac{f_c l}{2 v R_K} \qquad [19]$$

From the equation of focus it follows that

$$c = \frac{f_c}{1 - \frac{2 v R_K}{l}} \qquad [20]$$

Therefore the maximum admissible magnification of the light source is

$$\beta'_{max} = \frac{c'}{c} = \frac{l}{2 v R_K} - 1 \qquad [21]$$

For l = 6000 mm (236.22 inches), R_K = 150 mm (5.90 inches), and the aperture ratio v = 3.1, the enlargement β'_{max} is accordingly 5.45 times the original.

If lateral extension of the light source is required, the condition of equal aperture for rays near the axis does not suffice to attain uniform brightness in the image field. For a point of light located to the side of the axis, a supplementary, artificial vignetting occurs. Figure 20 will serve to illustrate. The free apertures are here so chosen as to produce

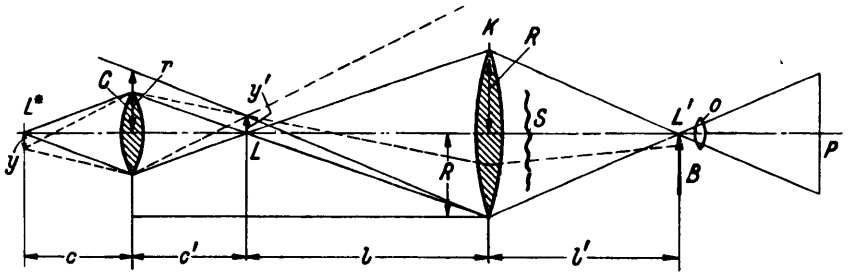

Figure 20 - For Lateral Extension of the Light Source the Illuminating System Must Have a Larger Aperture within the Schlieren Arrangement

exactly the same aperture for the axial point with respect to the condenser C and the schlieren objective K. The figure clearly shows that the schlieren objective K is not completely illuminated for a point of light distant from the axis. Therefore a sharper decrease of brightness occurs toward the edge than that stated by Equation [15]. Furthermore, for points of the schliere lying to one side, the general image of the light source is rather screened off by the schlieren stop. Whereas a linear function of the brightness continues to exist for schlieren points in the axis, with respect to all occurring deflections, the linear range for certain values of ϵ can already be exceeded for points which are distant from the axis. To obviate these disadvantages, the aperture of the system of illumination must be larger than that of the schlieren objective. Namely, the schlieren objective must continue to be completely illuminated by the outermost point of the effective light source (distance from the axis y is adjustable by the stop at L), i.e., the radius of the condenser C must equal r; see Figure 20. Then

$$\frac{R+r}{R+y'}=\frac{c'+l}{l} \qquad [22]$$

Now if $y' = \beta' y$, the equation of focus $c' = f_c\,(1 + \beta')$ and the definition of the aperture ratio $r = f_c/2v$ are taken additionally, then β', y', and f_c can be substituted for c', r, and y' in Equation [22].

$$\beta' \leqq \frac{1}{2}\sqrt{\left(\frac{R}{y}+\frac{l}{f_c}+1\right)^2+\frac{2l}{vy}-\frac{4R}{y}}-\frac{1}{2}\left(\frac{R}{y}+\frac{l}{f_c}+1\right) \qquad [23]$$

Now if the maximum permissible enlargement is calculated from Equation [23] for the previously used example, where l = 6000 mm (236.22 inches), R = 150 mm (5.90 inches), v = 3.1, and f_c = 130 mm (5.12 inches), then as a function of y = 1, 2, 4, and 8 mm, (0.0394, 0.0787, 0.1575, and 0.315 inch) we find that β' = 4.0, 3.3, 2.4, and 1.5 times the original.

The permissible enlargement is also a function of the focal length of the condenser. As Figure 21 shows, it is advantageous to select a condenser with the longest possible focal length. In practice, tests will have to be made to determine whether the condition expressed by Equation [23] is satisfied. For this purpose, one edge of the stop at L is moved toward the fixed one opposite it until only a small slit remains. In this case also, the schlieren objective must still be completely illuminated. The same is necessary also when the position of the edges is reversed. To conveniently perform this test, a stop will be used at L, which consists of four individually adjustable knife edges.

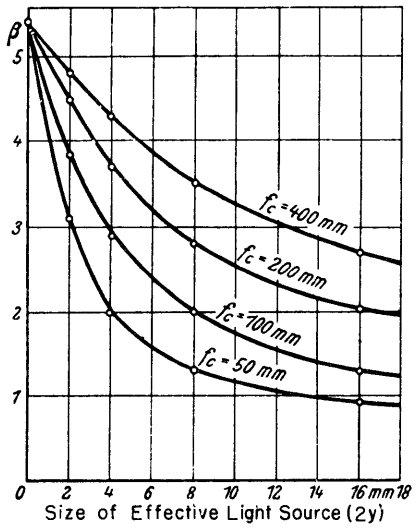

Figure 21 - Allowable Magnification of Effective Light Source as a Function of Focal Length of Condenser for Numerical Values Stated in Text

In Equation [15], which expresses the intensity of illumination in the image field P, introducing the condenser C changes nothing as long as the intensity of illumination of the condenser is sufficient to prevent artificial vignetting. The product $a'\,b'$ naturally becomes a function of the magnification β' of the intermediate image of the light source. Therefore the brightness increases as β'^2 without a schlieren stop. However, if so much light is screened off that the distance a' is kept constant, the intensity of illumination in the image field increases only linearly with β'.

A strong magnification is especially necessary if the distance a' is kept small to get sufficient brightness when adjusting to very weak schliere. Moreover, the size of the area of the light source which shows a sufficient uniformity of surface luminosity must be used as a criterion to determine β'. Hence, it will be favorable to have an optical train of very high light intensity always available for the condenser. Nevertheless, this requirement generally runs counter to that of errorless reproduction. Therefore, the effect which the image errors of the condenser C have will next be investigated.

The condenser C fully and completely answers its purpose if light rays are projected to all points on the schlieren objective from every point in the plane of the stop at L; see Figure 19. They need not all originate

from one point on the light source, but may belong to various points on the light source. In Figure 22, the cones of rays emanating from the two outermost points of the luminous surface are shown. If the point L_1^* together with the rays emanating from it is translated to L_2^*, then rays traverse every point in the space defined by L_1ML_2N which completely illuminate the schlieren objective K. For this reason, the plane of the stop does not absolutely need to be located at L_1L_2; it can be located somewhat ahead of or behind that position, but must lie in the space designated by L_1ML_2N. If so, the size of the surface which can be exploited is smaller, however. On the basis of these considerations, it can be predicted when the image errors of the condenser C will become disturbingly apparent. With respect to the chromatic error, there will be a different double cone L_1ML_2N for each color. For this reason a check must be made to determine whether the condition of Equation [23] is still satisfied for all colors. Otherwise, the usable range must be decreased correspondingly. The only usable region wherein the stop can be placed is that which contains parts of all double cones. Naturally, this decreases the enlargement which can be used as shown by Figure 23. Correct illumination just mentioned might be tested by a slit in the lateral position and by successive insertion of various chromatic filters.

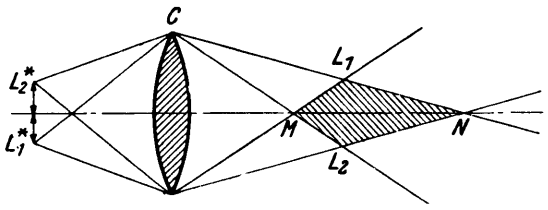

Figure 22 - Stop for Intermediate Image of Light Source Must Be Located in Space Defined by L_1ML_2N

C is the condenser, L_1^* and L_2^* are the two outermost lateral points of the light source.

Spherical aberration diminishes the space which can be utilized; see Figure 24. In the control mentioned, the harmful effect of spherical aberration would already have been recognized, for stopping down the illumination diaphragm to a slit in the outermost lateral position would have given no uniformly illuminated cone of rays. This would have had to be eliminated by decreasing the magnification to be exploited. Within the area $L_{11}M_1L_{22}N_1$ spherical aberration is no longer a disturbing factor.

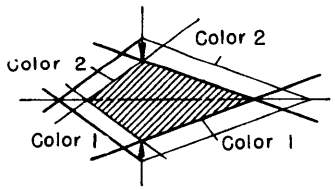

Figure 23 - Usable Space for Intermediate Image of Light Source with Consideration of Chromatic Error of Condenser

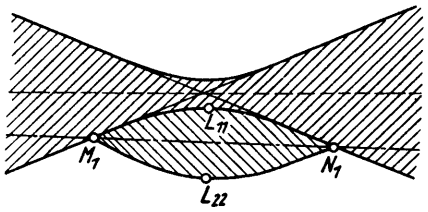

Figure 24 - Usable Space for the Stop

The area $L_{11}M_1L_{22}N_1$ is the usable space for the stop of the intermediate image of the light source when the area which is cross-hatched from the upper right to the lower left denotes the pencil of light rays emanating from the farthest lateral point at the bottom.

To diminish the path of light between the light source and the schlieren objective, a collecting lens often is inserted in the optical train of light. However, in such an arrangement it must be taken into account that errors in the lens affect the quality of the image of the light source. The collecting lens and the schlieren objective operate as the reproducing optical system. Since the latter will not be errorless if the collecting lens is chosen arbitrarily, decreased efficiency of this scheme must be taken in the bargain.

II. DEFLECTION OF LIGHT IN A NONHOMOGENEOUS, ISOTROPIC MEDIUM

1. THEORY OF LIGHT DEFLECTION IN A SCHLIERE

Applying Fermat's principle, we obtain

$$\frac{1}{R} = \frac{\text{grad } n}{n}^{\dagger} \sin \varphi \qquad [24]$$

where R is the radius of curvature of the light ray, see Figure 25, n is the index of refraction, and φ is the angle between grad n and the direction of the light ray. Equation [24] permits the calculation of the corresponding curve of the light rays for a given schliere. The schlieren method would offer the possibility of checking results obtained experimentally.†† Usually, however, the condition of the schliere is unknown, and the schlieren method is the means used to acquire some information on the shape of the schliere and its condition.

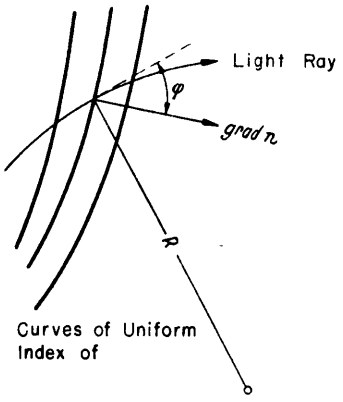

Figure 25 - Curvature of a Light Ray in a Nonhomogeneous Medium

It should be noted from the outset that, in general, a knowledge of the deflection of

† The gradient, here designated by grad n, denotes the maximum rate of change of n.

†† Compare "Dioptik in Medien mit kontinuierlich variablem Brechungsindex" (Dioptics in Media with Continuously Variable Index of Refraction), by R. Straubel, Handbuch der Physik, Winkelmann, Vol. 6, 1906, p. 485, and the studies by S. Exner and L. Matthiessen cited here.

light after passing through a schliere does not permit definite conclusions as to the condition of the schliere. A number of specific assumptions will at first have to be made if it is desired to determine the index of refraction $n(x,y,z)$ in reverse order from the values of the deflection.

For the investigation of phenomena in gases, the following observation offers simplification: The index of refraction depends only on the density ρ. In sufficient exactitude

$$\frac{n-1}{\varrho} = \text{const} \qquad [25]$$

i.e., $n = 1 + \text{const}\ \rho$.

For air, for example, $n = 1 + 0.000294\ \rho/\rho_0$, where ρ_0 denotes the density of air at zero degrees Centigrade and 760 mm Hg (29.92 inches Hg); n varies but very little with ρ. Not until $\rho/\rho_0 = 100$ does n deviate from n_0 by about three per cent. Therefore, for air

$$\text{grad}\ n = \frac{0.000\,294}{\varrho_0}\ \text{grad}\ \varrho \qquad [26]$$

For example if ρ increases by ρ_0 over a distance of 1 cm (0.394 inch), grad n = 0.000294/cm. From the foregoing, the radius of curvature of the light ray, $R = n/\text{grad}\ n = 1/0.0003 = 3300$ cm (1300 inches), when $\sin\varphi = 1$. Accordingly, in most cases the light ray within the schliere can be regarded as straight. As sufficient confirmation that it is permissible to consider all the light rays traversing a schliere as rectilinear, the following equation

$$R_{\min} = \frac{1}{\frac{\text{const.}}{\varrho_0}(\text{grad}\ \varrho)_{\max}} \gg d_{\max} \qquad [27]$$

can be written for the minimum radius of curvature of the light ray, where $d_{\max}$ denotes the outermost diameter of the schliere. However, this condition is not necessary. The magnitude $(\text{grad}\,\rho)_{\max}$ and therefore the curvature $1/R$ of the light ray may very probably assume large values, if only the corresponding segment of travel of the light ray is sufficiently small.

Let it be assumed that according to Figures 26 and 27 a light ray impinges at the point $y_0\ z_0$ parallel to the x-axis on the schliere to be examined and that its course within the schliere can be regarded as practically rectilinear. Then at a point on the light ray within the schliere for the plane of grad n and the linear element of the light ray at this point, which practically equals dx,

$$\left.\begin{aligned} \eta' &= 0 \\ \eta'' &= \frac{\text{grad}\ n}{n}\sin\varphi \end{aligned}\right\} \qquad [28]$$

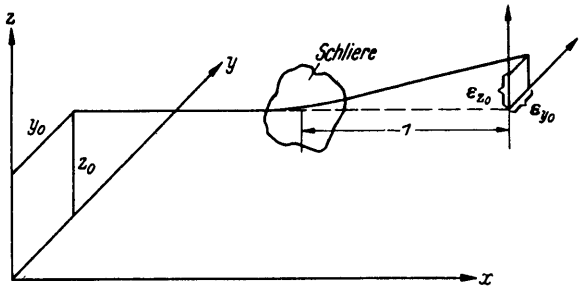

Figure 26 - The Deflection ϵ_{z_0}, ϵ_{y_0}, Measured in Radians for the Point $y_0 z_0$ of the Schliere

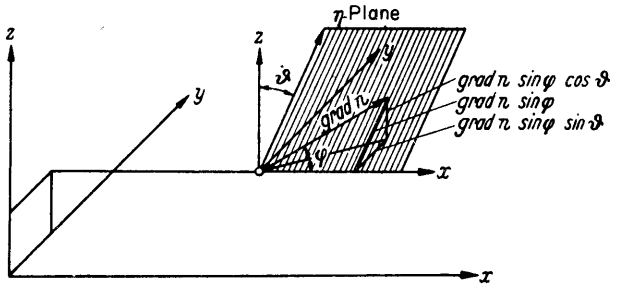

Figure 27 - Analysis of grad n

In the foregoing, η signifies the coordinate in this plane perpendicular to the x-axis, η' and η'' denote the first and second derivatives of η, and φ the angle of slope of grad n with respect to the x-axis.

Let the angle of slope of the η-x plane with respect to the z-x plane be ϑ, then

$$\left.\begin{aligned} z &= \eta \cos\vartheta & y &= \eta \sin\vartheta \\ z' &= \eta' \cos\vartheta & y' &= \eta' \sin\vartheta \\ z'' &= \eta'' \cos\vartheta & y'' &= \eta'' \sin\vartheta \end{aligned}\right\} \qquad [29]$$

and then

$$\left.\begin{aligned} y'' &= \frac{\text{grad } n}{n} \sin\varphi \sin\vartheta \\ z'' &= \frac{\text{grad } n}{n} \sin\varphi \cos\vartheta \end{aligned}\right\} \qquad [30]$$

The following relationships can be made from Figure 27

$$\left.\begin{aligned} \text{grad } n \sin\varphi \cos\vartheta &= \frac{\partial n}{\partial z} \\ \text{grad } n \sin\varphi \sin\vartheta &= \frac{\partial n}{\partial y} \end{aligned}\right\} \qquad [31]$$

Furthermore, for all cases where n is a factor in the equations, the index of refraction n_0 which is outside of the schliere can be substituted for n. This is permissible because the variation of n is so small that no appreciable error is thus produced. Therefore

$$\left.\begin{aligned} y'' &= \frac{1}{n_0} \frac{\partial n}{\partial y} \\ z'' &= \frac{1}{n_0} \frac{\partial n}{\partial z} \end{aligned}\right\} \qquad [32]$$

Since the light ray has been assumed straight for practical purposes, y'' and z'' continue to be functions of x only. Hence the angular deflection of the light ray, impinging parallel to the x-direction, produced by the schliere at the point $y_0 z_0$ is expressed

$$\left.\begin{aligned}\varepsilon_{y_0} = (y')_{x_2} &= \frac{1}{n_0}\int_{x_1}^{x_2}\left(\frac{\partial n}{\partial y}\right)_{x,\,y_0,\,z_0} dx \\ \varepsilon_{z_0} = (z')_{x_2} &= \frac{1}{n_0}\int_{x_1}^{x_2}\left(\frac{\partial n}{\partial z}\right)_{x,\,y_0,\,z_0} dx\end{aligned}\right\} \qquad [33]$$

where $x_1\, y_0\, z_0$ denotes the point of entry of the light ray into the schliere, and $x_2\, y_0\, z_0$ represents the point of exit.

2. CYLINDRICAL FIELD

If the condition on parallels to the x-axis becomes constant within the schliere, then according to Equation [33]

$$\varepsilon_y = \frac{1}{n_0}\left(\frac{\partial n}{\partial y}\right)_{y_0 z_0} l_s, \qquad \varepsilon_z = \frac{1}{n_0}\left(\frac{\partial n}{\partial z}\right)_{y_0 z_0} l_s \qquad [34]$$

where l_s denotes the distance traversed by the light ray within the schliere. With the help of these equations, therefore, $\partial n/\partial y$ and $\partial n/\partial z$, i.e., grad n, can be stated at every point (x,y) for a cylindrical field on the basis of measurements with the help of the schlieren method. The index of refraction itself is obtained at the point $y_0 z_0$ by integrating in the y-direction from the outer space to the point in question, i.e.,

$$\int_{y_a}^{y}\frac{\partial n}{\partial y}\,dy \qquad [35a]$$

and correspondingly along the z-direction as follows

$$\int_{z_a}^{z}\frac{\partial n}{\partial z}\,dz \qquad [35b]$$

and by adding these integrals to the value n_0 of the external space. Therefore,

$$n_{(y\,z)} = n_0 + \frac{n_0}{l_s}\int \varepsilon_y\, dy$$

or

$$\frac{\Delta n}{n_0} = \frac{1}{l_s}\int \varepsilon_y\, dy \qquad \frac{\Delta n}{n_0} = \frac{1}{l_s}\int \varepsilon_z\, dz \qquad [36]$$

The principle of the arrangement which must be used to investigate a cylindrical field is shown in Figure 28. A practical example will be treated later. Let the field to be investigated, for example the temperature field about a horizontal heating pipe, lie at S and have an extent in depth

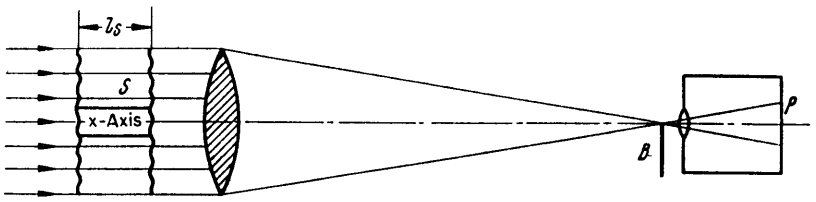

Figure 28 - Principles of the Schlieren Arrangement for Investigating a Cylindrical Field

l_s. Moreover, let it be illuminated by a pencil of parallel rays which has its focal point at B, i.e., the location of the schlieren stop. Furthermore, let the image of the schliere be located at P. Since the light rays do not traverse the schliere exactly rectilinearly to leave it with a deflection ϵ, but have a constant curvature, the problem arises regarding the distance at which P must be sharply focused to get a schlieren image which can be evaluated. If the light rays are assumed in first approximation to be arcs which have a very small inclination with respect to the x-axis and a very slight curvature, all light rays appear to emanate from the center of the field to be examined. Therefore, sharp focus of the latter, i.e., the center of the field, is requisite. A reliable index of correct focus is given by the fact that no schliere may be seen at P without a schlieren stop. Occasionally a position where the schliere completely disappears will not be found at all. This may be traced to the fact that the gradient of the index of refraction changes sharply and that the light rays are consequently not arcs. In this case, the plane of focus differs from point to point.

To decrease the resultant error to a minimum value, the reproduction by the lens O must be such that a maximum possible definition in depth results. In other words, according to Figure 29, the circle of dispersion δ on the plate P must be as small as possible in ratio to the size of the image when the object A is shifted by an amount Δ.

It is found that

$$\frac{\delta}{\beta} = -\frac{D\Delta}{s-\Delta}^{\dagger} \qquad [37]$$

---

† Derivation using the usual designations of optics:

$$xx' = -f'^2; \quad FA = x; \quad F'A' = x'; \quad A'B' = \frac{f'^2}{x-\Delta} - \frac{f'^2}{x}; \quad \delta = \frac{DA'B'}{f' + \frac{f'^2}{x-\Delta}};$$

$$\frac{\delta}{\beta} = \frac{D\frac{\frac{f'^2}{x-\Delta} - \frac{f'^2}{x}}{f' + \frac{f'^2}{x-\Delta}}}{-\frac{f'}{x}} = -\frac{D\Delta}{x-\Delta+f'}; \quad x \approx s - f';$$

from the foregoing

$$\frac{\delta}{\beta} = -\frac{D\Delta}{s-\Delta}.$$

Accordingly, the definition in depth is independent of the focal length of the lens. The longer the schliere is, and furthermore, the larger D is, i.e., the stronger the light deflection at the position of the schlieren stop, the greater δ/β becomes. The diameter of the lens is only valid, naturally, to the extent that light actually falls upon it.

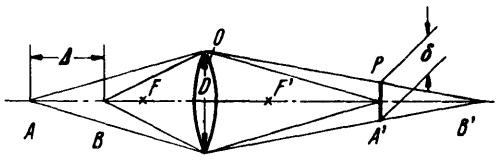

Figure 29 - Arrangement for the Evaluation of the Definition in Depth

To make δ/β small, the definition in depth Δ will be kept small, therefore, and the deflection ϵ will also be smaller. To achieve sufficient sensitivity in spite of this, the distance s can be taken sufficiently large. However, both are possible only to a certain limit: A sharp decrease of Δ is hence inadmissible because the assumptions for cylindrical condition of distribution are no longer valid in consequence of the edge effects. Moreover, for technical reasons, s cannot be made sufficiently large to maintain the requisite sensitivity at all times.

As is so often necessary, a middle course must be taken. The best criterion for satisfactory results is the occurrence of a uniform distribution of brightness on the ground glass without a schlieren stop.

If required the sensitivity can be approximately doubled by using the principle of the coincidence method. This arrangement may be practically achieved if a plane mirror is installed at the left side of the pencil of rays in the apparatus shown in Figure 28. This mirror, moreover, is placed so that it almost reflects the light emanating from a prism at B back to the prism. The design of the light source is the same as that shown in Figure 11.

3. ROTATIONALLY SYMMETRICAL FIELD

The path of the light rays will be assumed practically rectilinear for the rotationally symmetrical field also. Equation [33] will be used as a basis for evaluation. Then, according to Figure 30,

$$\varepsilon_{y_0} = \frac{1}{n_0}\int \left(\frac{\partial n}{\partial y}\right)_{x, y_0, z_0} dx \qquad \varepsilon_{z_0} = \frac{1}{n_0}\int \left(\frac{\partial n}{\partial z}\right)_{x, y_0, z_0} dx$$

Moreover

$$\frac{\partial n}{\partial y} = \frac{\partial n}{\partial r}\frac{\partial r}{\partial y}; \quad r = \sqrt{x^2+y^2}; \quad \frac{\partial r}{\partial y} = \frac{y}{r}$$

for when

$$dy = 0, \quad dx = \frac{r}{x}\,dr \quad (\text{from } r\,dr = x\,dx + y\,dy)$$

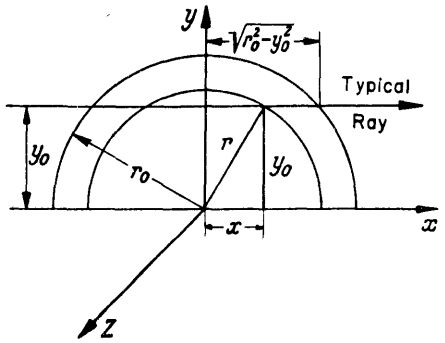

Figure 30 - Section through a Rotationally Symmetrical Field

The z-axis is the axis of symmetry; the x-axis is the optical axis.

Therefore

$$\varepsilon_{y_0} = \frac{2}{n_0} \int_{y_0}^{r_0} \frac{\partial n}{\partial r} \frac{y_0}{\sqrt{r^2 - y_0^2}} dr \qquad [38a]$$

and

$$\varepsilon_{z_0} = \frac{1}{n_0} \int \frac{\partial n}{\partial z} dx = \frac{2}{n_0} \int_{y_0}^{r_0} \frac{\partial n}{\partial z} \frac{r}{\sqrt{r^2 - y_0^2}} dr \qquad [38b]$$

where $2r_0$ is the diameter of the schliere in the plane $z = z_0$.

If the function of distribution for n were given, ϵ_y and ϵ_z could be calculated for every point. Here, however, with the aid of the schlieren method, ϵ is to be experimentally determined, and then the function $n = f(r,z)$ is to be determined by reverse calculation. For this purpose, the plane $z = z_0$ will be divided into a series of concentric rings which are so constructed that $\partial n/\partial r$ and $\partial n/\partial z$ can be assumed constant within each ring; see Figure 31. Let these values be

$$\left(\frac{\partial n}{\partial r}\right)_\lambda = \mu_\lambda \text{ and } \left(\frac{\partial n}{\partial z}\right)_\lambda = \nu_\lambda$$

for the λth ring.

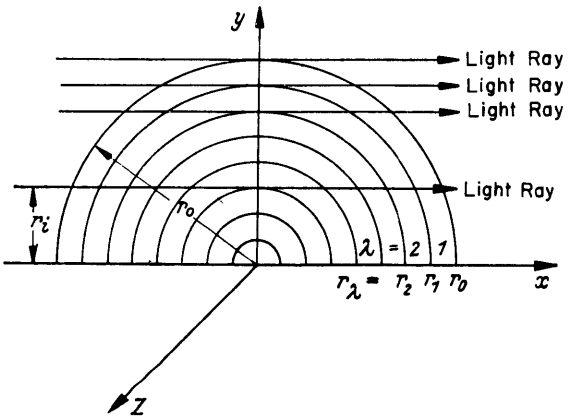

Figure 31 - Division of a Section in the Rotationally Symmetrical Field into Concentric Rings

The integrals for the deflection of the ith light ray can then be split up into a sum of individual integrals where μ or ν can be taken before the integral sign in every individual integral. Equation [38] becomes

$$\varepsilon_{y_0} = \frac{2r_i}{n_0} \sum_{\lambda=1}^{i} \mu_\lambda \left[\operatorname{Ar\,Cof} \frac{r_{\lambda-1}}{r_i} - \operatorname{Ar\,Cof} \frac{r_\lambda}{r_i} \right] \qquad [39]$$

correspondingly

$$\varepsilon_{z_0} = \frac{2r_i}{n_0} \sum_{\lambda=1}^{i} \nu_\lambda \left[\sqrt{\frac{r_{\lambda-1}^2 - r_i^2}{r_i^2}} - \sqrt{\frac{r_\lambda^2 - r_i^2}{r_i^2}} \right] \qquad [40]$$

The numerical evaluation of these integrals for ten concentric rings gives the numerical values in Table 1 and Table 2. The procedure of evaluation is as follows: ϵ_{y_0} and ϵ_{z_0} are determined for the first light ray. Since the geometrical dimensions are known, μ_1 and ν_1 are to be calculated from

TABLE 1

Values for $\epsilon_{y_0} \frac{n_0}{2r_i}$

Ray	
1	$0.467\mu_1$
2	$0.198\mu_1+0.495\mu_2$
3	$0.157\mu_1+0.211\mu_2+0.528\mu_3$
4	$0.137\mu_1+0.167\mu_2+0.225\mu_3+0.570\mu_4$
5	$0.124\mu_1+0.146\mu_2+0.180\mu_3+0.245\mu_4+0.622\mu_5$
6	$0.116\mu_1+0.134\mu_2+0.158\mu_3+0.197\mu_4+0.269\mu_5+0.693\mu_6$
7	$0.111\mu_1+0.126\mu_2+0.146\mu_3+0.174\mu_4+0.218\mu_5+0.304\mu_6+0.795\mu_7$
8	$0.107\mu_1+0.122\mu_2+0.138\mu_3+0.162\mu_4+0.196\mu_5+0.250\mu_6+0.355\mu_7+0.962\mu_8$
9	$0.106\mu_1+0.118\mu_2+0.135\mu_3+0.156\mu_4+0.186\mu_5+0.229\mu_6+0.300\mu_7+0.446\mu_8+1.317\mu_9$

TABLE 2

Values for $\epsilon_{z_0} \frac{n_0}{2r_i}$

Ray	
1	$0.484\nu_1$
2	$0.235\nu_1+0.515\nu_2$
3	$0.212\nu_1+0.255\nu_2+0.553\nu_3$
4	$0.215\nu_1+0.236\nu_2+0.281\nu_3+0.601\nu_4$
5	$0.235\nu_1+0.248\nu_2+0.269\nu_3+0.317\nu_4+0.663\nu_5$
6	$0.276\nu_1+0.284\nu_2+0.296\nu_3+0.318\nu_4+0.368\nu_5+0.750\nu_6$
7	$0.352\nu_1+0.356\nu_2+0.364\nu_3+0.376\nu_4+0.399\nu_5+0.451\nu_6+0.882\nu_7$
8	$0.512\nu_1+0.514\nu_2+0.519\nu_3+0.526\nu_4+0.537\nu_5+0.559\nu_6+0.614\nu_7+1.118\nu_8$
9	$1.006\nu_1+1.007\nu_2+1.009\nu_3+1.012\nu_4+1.017\nu_5+1.026\nu_6+1.045\nu_7+1.096\nu_8+1.732\nu_9$

Equations [39] and [40]. For the first light ray, the sum contains only one term. Since μ_1 and ν_1 are now known, the equations for the second light ray contain only one unknown term each, i.e., μ_2 and ν_2, etc. In this way, values of $\partial n/\partial r$ and $\partial n/\partial z$ can be determined for each ring zone successively. The refraction itself at a point is found by integrating in the direction of the radius r or in the direction of the z-axis:

$$\left.\begin{aligned} n(r,z) &= \int_{r=r_a}^{r} \left(\frac{\partial n}{\partial r}\right)_z dr + n_0 \\ \text{or} \qquad n(r,z) &= \int_{z=z_a}^{z} \left(\frac{\partial n}{\partial z}\right)_r dz + n_0 \end{aligned}\right\} \qquad [41]$$

r_a or z_a is that r- or z-coordinate to which the schliere extends; there $n = n_0$.

If the values ϵ_{y_0} and ϵ_{z_0} have been determined for a phenomenon which is to be investigated, $n = f(r,z)$ can be calculated in two ways. This furnishes a possibility for checking the correctness of measurement or calculation and the accuracy of the method.

III. MEASUREMENT OF LIGHT DEFLECTIONS

1. GRID-SCREEN METHOD

A simple method for quantitative measurement of the light deflection for every point of the schliere is as follows: A narrow slit is chosen as a light source, and a grid whose grid constant is $2a$ is used as a schlieren stop. The light which is not deflected is permitted to just traverse a free aperture of the grid. A darkening of the image in the schliere is produced for all points of the schliere which deflects the light by the amount a on the grid, perpendicular to the direction of the grid bars. In contrast, all points which deflect the light by $2a$ are bright, whereas those which deflect it by $3a$ are dark, etc. Thus curves for a constant deflection in a definite direction are obtained in the image of the schliere. These curves will be designated as isophotes (Isophoten), since according to Section 2, the brightness must be constant along these curves in a normal schlieren photograph, i.e., with a single knife edge. Depending directly on the direction of the grid, ϵ_y or ϵ_z equals a definite amount along the curves. This amount depends upon the grid constant $2a$, the distance s of the grid from the schliere, and ordinal number k. The symbol k is the number of the aperture through which the light falls for a given curve, calculated from the passage of the direct rays. It is found that

$$\varepsilon = k\frac{2a}{s} \qquad [42]$$

where a and s are magnitudes which can be measured directly and k can be stated immediately in many cases, for example, if it is known that the variation of the index of refraction from the external space must be constant, the succession of curves obtained corresponds to that of the ordinal numbers insofar as no closed curves are present for which in turn a decrease of the

ordinal number might occur. In indeterminate cases the ordinal number to which a given curve corresponds can be determined experimentally by screening off the light in front of the grid. This will be illustrated by two examples.

Figures 32 and 33 show the curves of constant deflection as produced by a horizontal heating pipe. More specifically, Figure 32 gives the curves of constant deflection in a horizontal direction which will here be selected as the z-axis, and Figure 33 gives those in a vertical direction (ϵ_y). The diameter of the heating pipe was 40 mm (1.57 inch) and its length was 555 mm

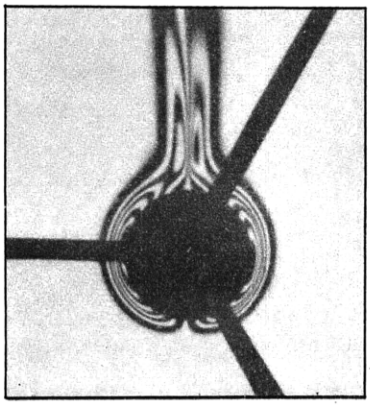

Figure 32 - Curves of Constant Deflection in Horizontal Direction, Produced by a Horizontal Heating Pipe in Otherwise Undisturbed Air

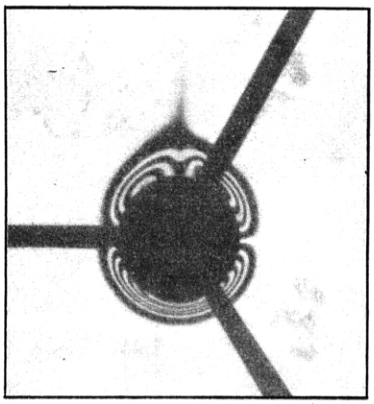

Figure 33 - Curves of Constant Deflection in Vertical Direction for the Temperature Field of a Horizontal Heating Pipe

The three stripes emanating from the shadow photograph of the heating pipe are produced by the brackets holding the pipe.

(21.85 inches). The photograph was taken by the method shown in Figure 18 in order to use a parallel beam of light rays. The distance between the bars in the grid screen was 5 mm (0.197 inch). The focal length of the concave mirror was 3.625 m (11.89 feet). Therefore, for the first curve, i.e., for that one produced by the light deflected by a distance equal to the grid constant, calculated from the outside inward

$$\varepsilon_y \quad \text{or} \quad \varepsilon_z = \frac{5}{3625} = 0.00138$$

Therefore, based on Equation [34], along the isophotes

$$\frac{\partial n}{\partial y} = \frac{n_0 \varepsilon_y}{l_s} = k \frac{0.00138}{55.5} \text{ cm}^{-1} = k \cdot 0.0000249 \text{ cm}^{-1}$$

and likewise

$$\frac{\partial n}{\partial z} = k \cdot 0.0000249 \text{ cm}^{-1}; \quad k = 1, 2, 3 \ldots$$

For purposes of evaluation, the values for $\partial n/\partial z$ for horizontal straight lines are taken from Figure 32; these are plotted in Figures 34 and 35. Curve 1 is the deflection for that horizontal line which touches the lower side of the heating pipe. Curve 7 touches the upper side; between them lie the horizontals which divide the perpendicular diameter into six equal parts. Above the pipe, Curves 8 to 10 follow each other equidistantly.

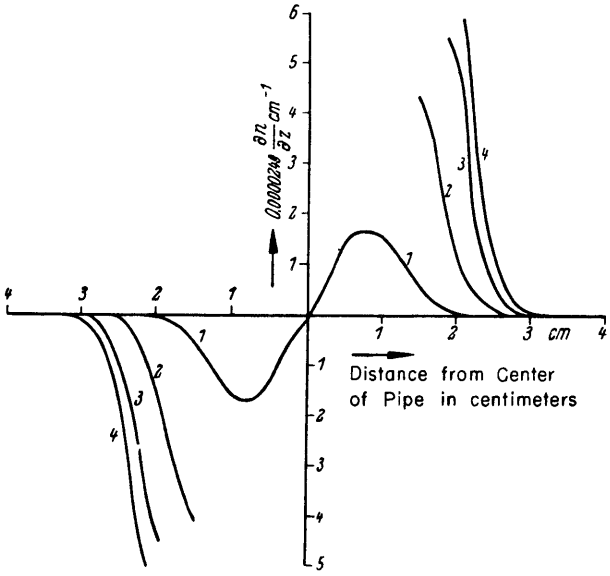

Figure 34 - Plotted Values of the Data for $\partial n/\partial z$ for Plane Horizontal Sections Taken from Figure 32

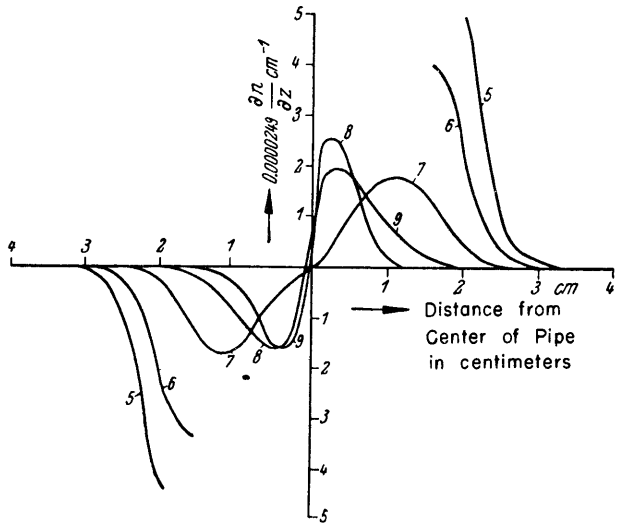

Figure 35 - Plotted Values of the Data for $\partial n/\partial z$ for the Upper Side of the Heating Pipe

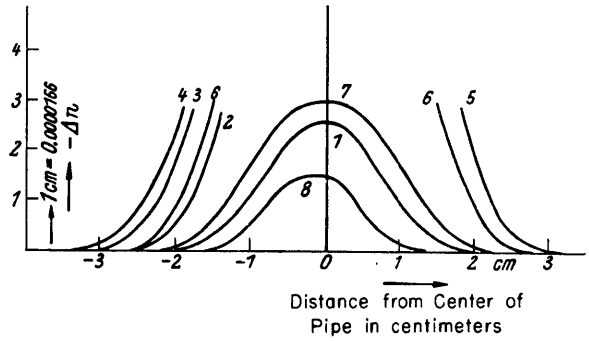

Figure 36 - Variation of the Index of Refraction Δn for the Horizontal Plane Sections Produced by the Temperature Field of a Horizontal Heating Pipe

Integration of these curves gives

$$\Delta n = \int_{z_a}^{z} \frac{\partial n}{\partial z} dz$$

where Δn is the amount by which the index of refraction of the external space is changed; Δn is plotted in Figure 36.

By integrating through along the entire line, the external values n_0 of the index of refraction must result, i.e., the positive and negative areas of the curves in Figures 34 and 35 must be equal. This permits good checking of the accuracy.

If it is desired additionally to convert from the refraction index to the temperature, the relationship expressed by Equation [24] is used, i.e., $(n - 1)/\rho$ = constant. For the present case, therefore

$$\left.\begin{aligned} &\frac{n_0 - 1}{n_0 + \Delta n - 1} = \frac{\varrho_0}{\varrho_0 + \Delta \varrho} = \frac{T_0 + \Delta T}{T_0} \\ &\Delta T = \frac{T_0}{n_0 + \Delta n - 1}(-\Delta n) \end{aligned}\right\} \qquad [43]$$

As Δn is negative, the temperature rise ΔT becomes positive. T_0 denotes the absolute temperature which corresponds to the density ρ_0.

Photographs of a glass plate are here reproduced as a second example for the use of the grid screen. These photographs do not permit the ordinal numbers of individual isophotes to be determined directly. Therefore, two photographs were made, Figures 37 and 38. In Figure 37 a grid having a

Figure 37

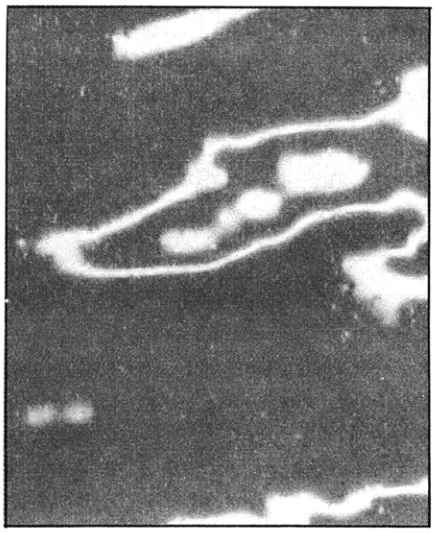

Figure 38

Figures 37 and 38 - Schlieren Photographs of an Ordinary Glass Plate Using a Grid Screen

In Figure 38 the grid is partially covered.

grid constant of 4 mm (0.158 inch) was used as a schlieren stop; in Figure 38 the grid was covered from the side sufficiently to permit passage of the direct light only and of that light refracted toward the other side. Therefore, a few of the curves drop out of the photograph in Figure 38. Those which

disappear have the ordinal numbers -1, and under certain conditions also -2, -3, etc. Those remaining whose ordinal numbers are 0, +1, etc., are visible. By this method, determination of the ordinal number for the individual isophotes is possible. Since it must be assumed that the irregular deflection of the light by the glass plate is not founded on a change of the index of refraction but is due to the variation in thickness of the plate, the variation in thickness at every point can consequently be calculated from the photographs.

If the glass plate is held perpendicular to the parallel beam of light

$$\frac{\delta+\varepsilon}{\delta}=n;\ \text{hence}\ \ \delta=\frac{\varepsilon}{n-1} \qquad [44]$$

in first approximation. In Equation [44] δ is the wedge angle (Keilwinkel) of the plate at one point, and ϵ is the deflection of the light in the direction of greatest deviation; see Figure 39. Moreover $\epsilon_y = \epsilon \cos\beta$, where β denotes the angle between the direction of maximum deviation and the y-direction. Correspondingly $\epsilon_z = \epsilon \sin\beta$; therefore

$$\delta=\frac{\varepsilon_y}{(n-1)\cos\beta}=\frac{\varepsilon_z}{(n-1)\sin\beta} \qquad [45]$$

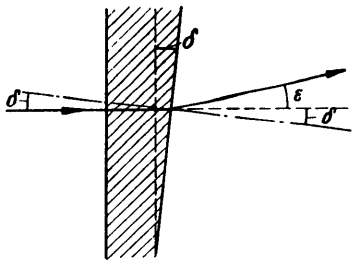

Figure 39 - Light Deflection by a Glass Wedge

δ is the wedge angle and the angle of incidence for the reverse face of the plate. $\delta + \epsilon$ is the angle of departure.

The thickness d itself is determined by integration:

a. Along the y-direction, where z = constant, it is expressed

$$d=d_0+\int_{y_0}^{y}\delta\cos\beta\,dy=d_0+\frac{1}{n-1}\int_{y_0}^{y}\varepsilon_y\,dy \qquad [46]$$

where d_0 is the thickness pertaining to y_0; or

b. Along the z-direction, where y = constant, it is expressed

$$d=d_0+\int_{z_0}^{z}\delta\sin\beta\,dz=d_0+\frac{1}{n-1}\int_{z_0}^{z}\varepsilon_z\,dz \qquad [47]$$

2. ADJUSTABLE SLIT STOP

In place of a grid screen, a slit can be installed in the location of the schlieren stop. This slit can be shifted according to measured values. This produces only one isophote each time. However, as the position of the slit stop can be changed, the entire field can be measured little by little.

For objects which do not vary with time, successive photographs at different positions of the slit stop can be taken or the position of the isophotes can be measured directly with a measuring microscope.

For variable phenomena, apparatus for shifting the slit stop can be coupled to the driving mechanism of a motion-picture camera. This permits taking a rapid succession of photographs.

3. MEASUREMENT OF BRIGHTNESS AND COMPARISON WITH A STANDARD SCHLIERE

On page 6, it was determined that the brightness in the image field is proportional to the deflection in the schliere, considering the assumptions there made. Accordingly, it is therefore possible to determine the deflection in reverse order from the brightness. Consequently the brightness could be measured from point to point with a photometer, and the deflection in the corresponding points on the schliere could be calculated from Equation [16]. If Equation [16] is written in the form

$$E^* = \eta \mathfrak{B} \frac{b'}{t^2} (a' + \Delta a')$$

where $\Delta a'$ is to be interpreted as the deflection of the image of the light source at the schlieren stop, produced by one point on the schliere, then

$$E^* = \eta \mathfrak{B} \frac{b'}{t^2} (a' + \varepsilon s) \qquad [48]$$

$$\varepsilon = \frac{t^2}{\eta \mathfrak{B} b' s} E^* - \frac{a'}{s}$$

For this purpose, the absolute values of t, $\mathfrak{B}$, b', η, s, and a' must be known. Furthermore, the condition during the time required for measurement must not change. Hence only stationary phenomena are concerned.

The evaluation becomes simpler and can also be applied to known stationary phenomena if the schlieren image is photographed and a standard schliere which produces calculable deflections is photographed simultaneously. Comparison of the blackening in the object and in the standard schliere gives the value of the deflections ϵ without exact knowledge of the absolute values of the foregoing magnitudes.

This method is best applicable if the light deflection in the schliere is not large enough to permit use of a grid screen. To get the isophotes at small values of ϵ, the distance between the grid bars would have to be so small that as a result of the diffraction about the bars a satisfactory image of the object would no longer be produced.

A plano-convex lens of very small curvature can be used as a standard schliere. Its curvature must have such a value that the deflection of the

ray traversing it at the edge is equal to or somewhat larger than the maximum deflection in the phenomenon. The order of magnitude is 0.001 radian.

The radius of curvature of such a slightly arched lens can only be determined with the aid of Newton's rings.

A ray of light which impinges perpendicularly on the plane surface of the standard schliere with a focal length of f' from a distance of 1 cm (0.394 inch) from the axis is deflected by the curved surface by an amount $1/f'$. Correspondingly the deflection for a distance δ cm from the axis is $\pm \delta \frac{1}{f}$. This permits a scale to be applied to the standard schliere which corresponds to definite values of the deflection. Deflection occurs in the direction toward the axis. However, because only the horizontal or the vertical deflection enters the problem with respect to the schlieren image, depending upon the position of the stop, the deflections for every point of the standard schliere must be given in a definite direction. An example of this is the x-direction in Figure 40. Let the deflection at the point P' be $\epsilon_0 x$. Then the deflection at P in the direction toward the midpoint 0 is $\frac{\epsilon_0 x}{\cos \varphi}$. However, the value of the deflection at P in the x-direction is

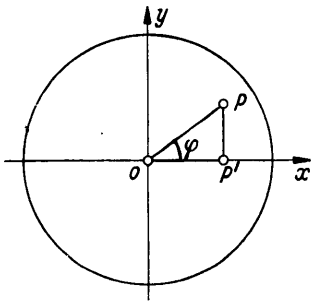

Figure 40 - For the Analysis of the Deflection by a Standard Schliere

$$\frac{\epsilon_0 x}{\cos \varphi} \cos \varphi = \epsilon_0 x$$

that is, deflection in the x-direction is constant at all points having equal values of x. Therefore, the isophotes of the standard schliere are straight lines parallel to the edge of the schlieren stop.

If convergent light rays impinge on a plane-parallel glass plate whose thickness is d, a displacement of all obliquely traversing rays occurs which results in a deflection of the point of convergence by about $d/3$. Hence, if such a plate is inserted into the convergent cone of Toepler's schlieren arrangement, a displacement of the position of the image point of the light source occurs for that portion of the rays traversing the plate. Therefore, the schlieren stop is not located at the right place with respect to the glass plate, if its position was determined without the glass plate; see Part I, Section 5. Even a completely plane-parallel plate produces a one-sided darkening of the image. Consequently the brightness is here not proportional to the angle variation alone. Hence, the standard schliere cannot be inserted into the convergent portion of the schlieren arrangement. However, a displacement of the rays does not

occur if parallel light impinges perpendicular to the plate. As a result, the standard schliere can be used only in the arrangements shown in Figures 9 and 18.

The brightness in the schlieren image, however, depends additionally on the losses of light in the glass plate.

With respect to the reflection losses for k interfaces of the mediums with the indexes of refraction n and n', the ratio of the penetrating light Φ_d to the incident light Φ_e is

$$\Phi_d/\Phi_e = (1-p)^k; \text{ where } p = \left(\frac{n'-n}{n'+n}\right)^2 \qquad [49]$$

For reflection at a glass-air interface, the indexes of refraction are n' = 1.5, n = 1, and p = 0.04 with close approximation. For two reflective surfaces, as for the standard schliere, therefore,

$$\Phi_d/\Phi_e = 0.96^2 = 0.9216$$

The losses by absorption are expressed

$$\Phi_d/\Phi_e = a^d \qquad [50]$$

where d is the path of light in millimeters.

a = 0.99952 for prism crown glass
a = 0.9992 for barium glass and flint glass.

Therefore, for a path of light of 8 mm (0.315 inch) in the standard schliere,

$$\Phi_d/\Phi_e = 0.9936^8 = 0.9949$$

The total loss of light in the standard schliere determines that only the fraction η' = 0.9216 × 0.9949 = 0.917 of the impinging light leaves the glass plate.

The brightness in the schlieren image of the standard schliere is correspondingly given by

$$E_n^* = \eta'\,\eta\,\mathfrak{B}\frac{b'}{t'}(a' + \varepsilon_n\, s) \qquad [51]$$

where ϵ_n signifies the deflection in the standard schliere.

Therefore, for two points in the schlieren image of the phenomenon to be investigated and of the standard schliere which are both of equal brightness,

$$a' + \varepsilon\, s = \eta'\,(a' + \varepsilon_n\, s) \qquad [52]$$

$$\varepsilon = \eta'\,\varepsilon_n - \frac{a'}{s}(1-\eta') \qquad [53]$$

By comparison of the brightness in the schlieren image, this formula permits calculation of the deflection at every point of the phenomenon. The sole remaining inconvenience is that the absolute value of a'/s is contained in Equation [53]. In spite of this, the following simplified evaluation is possible:

That point in the standard schliere is determined which shows the same brightness as the external image field where there is no deflection. Let the deflection of the desired point in the standard schliere be ϵ_{0n}. Then by Equation [53],

$$\left.\begin{aligned} 0 &= \eta' \varepsilon_{0n} - \frac{a'}{s}(1-\eta') \\ \frac{a'}{s} &= \frac{\eta'}{1-\eta'} \varepsilon_{0n} \end{aligned}\right\} \qquad [54]$$

In this way determination of the absolute value of a'/s can be avoided:

$$\varepsilon = \eta' \varepsilon_n - \eta' \varepsilon_{0n} = \eta' (\varepsilon_n - \varepsilon_{0n}) \qquad [55]$$

If the deflection in the standard schliere is set as $\epsilon_n = \epsilon_0 x$, where x is the component of the distance from the midpoint of the standard schliere perpendicular to the schlieren stop, then

$$\varepsilon = \eta' \varepsilon_0 (x - x_0) \qquad [56]$$

where x_0 is the point in the standard schliere which shows the same brightness as the external image field. If, furthermore, $\eta' \epsilon_0$ is designated by ϵ_0',

$$\varepsilon = \varepsilon_0' (x - x_0) \qquad [57]$$

Equation [57] serves as a basis for analysis. Therefore, the problem should be attacked in the following manner: First, that point in the standard schliere is determined which shows the same brightness as the undisturbed image field. This point will be considered the zero point in the standard schliere. Then the point will be sought which is of the same brightness as that point in the object whose deflection is to be measured. The desired deflection ϵ is then equal to the distance of this point from the zero point of the standard schliere, multiplied by the coefficient ϵ_0' pertaining to the standard schliere.

4. DETERMINATION OF THE DENSITY IN THE VICINITY OF A FLYING PROJECTILE

Figure 41 is a schlieren photograph of a flying projectile. The picture also shows the variation in brightness simultaneously produced by a standard schliere. The knife edge was horizontal. Correspondingly, the schliere about the flying projectile appear as though they were illuminated

from below. The variations in brightness are both positive and negative; the sharpest variations in brightness appear in the front of the head wave and tail wave. If the range of deflections encompassed by the standard schliere is insufficient to correspond to the greatest deflections present in the object, it is helpful if the light traversing the standard schliere can be deflected laterally by a small amount. This can be accomplished simply if the standard schliere has a small wedge error. Then the point which reveals the same brightness as the external optical field can be shifted as desired by rotating the standard schliere. If the axis of the projectile coincides with the direction of flight, the phenomenon of the flow about the projectile is rotationally symmetrical. Therefore, Equations [38], [39], and [40] are used for evaluation.

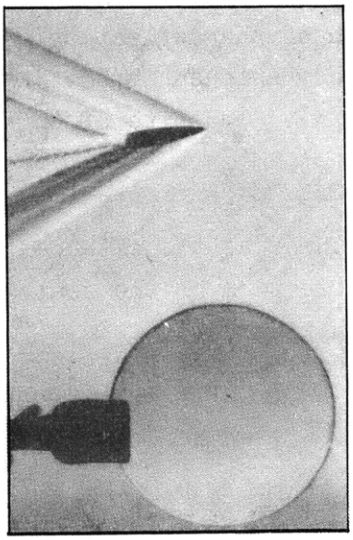

Figure 41 - Schlieren Photograph of a Flying Projectile with Simultaneous Reproduction of Standard Schliere

The values ϵ_y or ϵ_z are best obtained by a photogram, recorded with a recording photometer. Such a photogram is reproduced in Figure 42 for a cross section approximately through the middle of the projectile as seen in Figure 41. A corresponding photogram for the standard schliere furnishes a calibration of the ordinate values of the light deflection in radians. The values for ϵ_y, obtained by dividing the section into ten concentric circles, are then entered in the last line of Table 3. By multiplying by $n_0/2r_i$, the individual values follow for the summation of Equation [39]. In each case

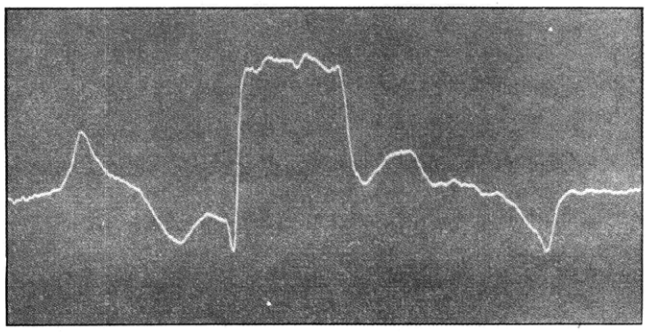

Figure 42 - Photogrammetric Plot of the Darkness in a Schlieren Photograph

TABLE 3

An Outline of the Numerical Calculation of the Variation in the Density of the Air in the Vicinity of a Flying Projectile, Taken from the Data Obtained from a Schlieren Photograph

This skeleton of the procedure in the numerical calculation is applicable to any schlieren problem having circular symmetry.

Ring	Ray 1		Ray 2		Ray 3		Ray 4		Ray 5		Ray 6		Ray 7		Ray 8		Ray 9		$\frac{\partial n}{\partial r}$	$\frac{\partial n}{\partial r}\Delta r$	$n_0 + \Sigma \Delta n$	$(n-1)\cdot\frac{\varrho_0}{n_0-1}$
1	0.467		0.198		0.157		0.137		0.124		0.116		0.111		0.107		0.106		μ_1	$(\Delta n)_1$	n_1	ϱ_1
2			0.495		0.211		0.167		0.146		0.134		0.126		0.122		0.118		μ_2	$(\Delta n)_2$	n_2	ϱ_2
3					0.528		0.225		0.180		0.158		0.146		0.138		0.135		μ_3			
4							0.570		0.245		0.197		0.174		0.162		0.156		μ_4			
5									0.622		0.269		0.218		0.196		0.186		μ_5			
6											0.693		0.304		0.250		0.229		μ_6			
7													0.795		0.355		0.300		μ_7			
8															0.962		0.446		μ_8			
9																	1.317		μ_9			
	$2r_1$	$\frac{n_0\varepsilon_1}{2r_1}$	$2r_2$	$\frac{n_0\varepsilon_2}{2r_2}$	$2r_3$	$\frac{n_0\varepsilon_3}{2r_3}$	$2r_4$	$\frac{n_0\varepsilon_4}{2r_4}$	$2r_5$	$\frac{n_0\varepsilon_5}{2r_5}$	$2r_6$	$\frac{n_0\varepsilon_6}{2r_6}$	$2r_7$	$\frac{n_0\varepsilon_7}{2r_7}$	$2r_8$	$\frac{n_0\varepsilon_8}{2r_8}$	$2r_9$	$\frac{n_0\varepsilon_9}{2r_9}$				
n_0	ε_1		ε_2		ε_3		ε_4		ε_5		ε_6		ε_7		ε_8		ε_9					

they are entered in the second division of the next to the last line of Table 3. Above them in the same column, the values of the summands for the individual rings should be inscribed. For Ray 1, the sum consists of one term only. Therefore, in the second division for Ray 1 and Ring 1, the value $n_0 \epsilon_1 / 2 r_1$ itself is to be entered. Dividing by a number obtained from Table 1, first division, first column, then gives $\frac{\partial n}{\partial r}$ for Ring 1. Thus all values for the first summands are calculable, i.e., the first line of the table is to be filled completely. Now in a corresponding manner $\left(\frac{\partial n}{\partial r}\right)_2$ is obtained by completing the term: Ray 2, Division 2, Ring 2. Then all values for the second ring are known, and so on. In this manner the evaluation becomes almost entirely mechanical.†

The values found for the density in the vicinity of the flying projectile agree well with those found with the aid of the interference refractor. Unfortunately, as a result of space limitations, it will be impossible to give more detailed data. This problem will be treated in a special article.

IV. LIMITS OF SENSITIVITY AND COMPARISON WITH OTHER METHODS

1. EFFECTS OF DIFFRACTION

The foregoing material was based on the assumption of geometric optics; however, certain phenomena can only be explained from the wave theory of light.

It is striking primarily in the observation of all sharp schlieren photographs that the edges of all objects are surrounded by a white margin resulting from diffraction. This white margin is absent only when the margin of the body is exactly perpendicular to the edge of the schlieren stop. For example, Figure 43 shows the facial profile edged in white. Furthermore, all the dust particles present on the mirror appear very sharply.

The origin of this phenomenon is to be sought in the diffraction of the light along the edge of the solid bodies. Based on Huygens' principle, light emanates from the latter when they are illuminated by a parallel beam of light. This light forms an angle of 90 degrees with the direction of the incident light, i.e., all edges function as deflectors, perpendicularly to the course of the edge. Therefore, even when the direct image of the light source is partially or completely screened by the schlieren stop, light from the edges still traverses the lens O. This explains the presence of an aura about all objects. Likewise all dust particles on the schlieren objective become strongly evident, for the arrangement then corresponds to normal, dark-field illumination of microscopes. Figure 44 is a photograph of a fine wire net which shines only in the diffracted light.

---

† Compare H. Schardin, Zeitschrift für Instrumentenkunde, Vol. 53, 1933, page 433.

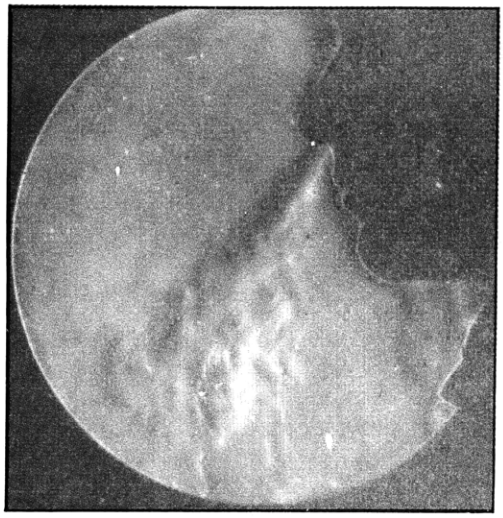

Figure 43 - Exhaled Warm Air Made Visible

The profile of the face is surrounded by a border resulting from diffraction. At the lower part of the optical field, a disturbance produced by non-uniform lacquering of the mirror is visible. The white points are caused by diffraction about dust particles.

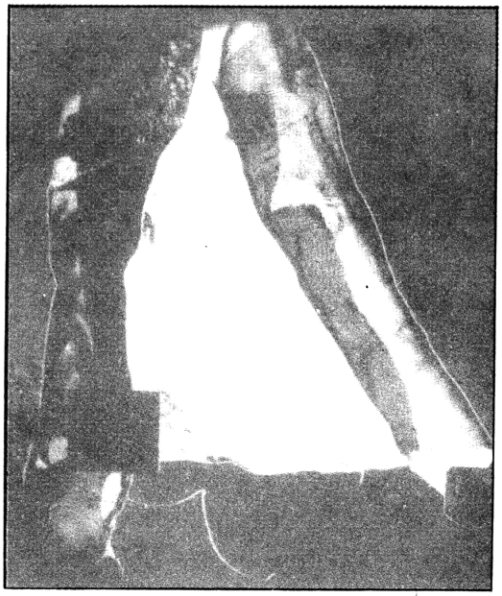

Figure 44 - Schlieren Photograph of a Wire Netting

All direct light is screened by the schlieren stop. The netting is only visible as a result of the light diffracted by the mesh.

The space of diffraction corresponds essentially to the so-called Beck light line visible in microscopes along narrow boundary layers of media of a varying index of refraction when illuminated by parallel light rays. The foregoing phenomenon, moreover, plays a certain part in optical measuring methods of crystallography.†

The diffraction along the edges of objects present in the objective space has no effect on results of the methods considered heretofore. The diffracted light is again collected along the edges of the images by the lens O. Hence, it does not disturb the brightness in the image of the schliere to be investigated. In contrast, the diffraction along the edges can be used advantageously to produce a sharp focus of the object as follows. A narrow, vertical strip of the light source is selected, and its image is so covered at the schlieren stop that the diffracted light can still pass on both sides. This is shown in Figure 45. On the ground glass, all objects are then in general surrounded by a double border of light. There is a single border of light only at the point of exact, sharp focus. The adjustment is very exact

† For example, see F. Rinne and M. Berek, "Anleitung zu Optischen Untersuchungen mit dem Polarisationsmikroskop," (Introduction to Optical Investigations with the Polarizing Microscope), Jänecke, Leipzig, 1934, page 201.

because the diffracting edge of the objects can be regarded as an infinitely thin line of light, and hence the point can be determined exactly where only a single line of light appears. A finite width of the border of light is determined only by the image error of the lens O. Under certain circumstances a new method to determine experimentally the image error of optical systems might be built up on this phenomenon.

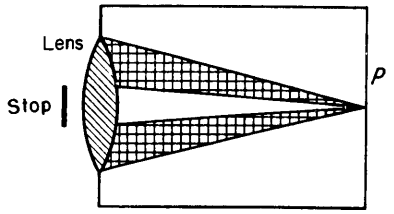

Figure 45 - For Sharp Focus on the Object Using the Border of Diffraction

The diffraction which occurs at the schlieren stop itself is unfavorable. In a very sensitive adjustment, the schlieren stop is placed very close to the edge of the image of the light source. Thus, for example, on page 8 a width a' for the admitted image of the light source of only 0.06 mm (0.00236 inch) was calculated. Now, if this width were regarded as a slit and if the parallel light were permitted to impinge on it, the first maximum value of the diffraction would be $\delta = 2\lambda/a'$ radians. When $\lambda = 0.0006$ mm (0.0000236 inch) and $a' = 0.06$ mm (0.00236 inch), $\delta = 0.02$. If the order of magnitude of this value $\delta = 0.02$ is also regarded as a scale for the lack of sharpness of objects with the schlieren arrangement actually present, it is found that the lack of sharpness $\delta = 0.02$ already constitutes a considerable fraction of the largest permissible total angle of the image field of about 8 degrees, which is equal to approximately 0.14 radian; see page 5. From this rough estimate, it is evident in any case that the diffraction at the schlieren stop must affect distribution of brightness in the image. Unfortunately, an exact investigation of this phenomenon has not been possible to the present. Even the physical condition in the image point is an incompletely solved problem as yet. Now an additional stop is inserted at the image point. At the image point of the light source, furthermore, the object which is to be reproduced must be optically contained in some way. Assuming a point source of light, naturally under ideal reproduction and without schlieren in the path of the rays, a point would be reproduced as the image point. Moreover, this point would be independent of the shape of the object present in the locale of the schliere. However, the contour of the object is still present on the ground glass. Hence, the image point of the light source could be compared to the reproductive cell of a living organism in which the entire future organic development is already contained.

Complete theoretical treatment of these complicated conditions would not be feasible at this point. Therefore, only a few test results will be reported.

With a very sensitive adjustment of the schlieren stop, where the schlieren stop is almost entirely shut, a dark shadow of diffraction perpendicular to the edge of the stop emanates from the margin of all objects located in a beam at the schliere; see Figure 46. It can be demonstrated that the diffraction along the edge of the schlieren stop is actually responsible for this because the shadow turns also when the stop is rotated.

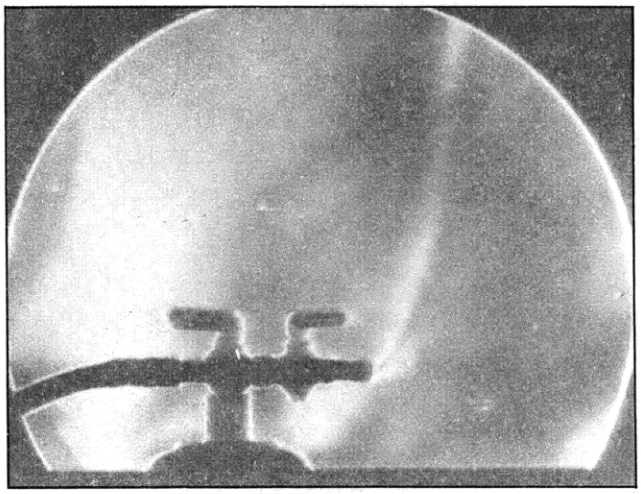

Figure 46 - Schlieren Photograph of Illuminating Gas Flowing from a Slightly Open Gas Cock, Made by the Coincidence Method

The amount of gas escaping was so small that the odor of the gas could not be perceived. The phenomena of diffraction about the gas cock should be noted.

Figure 47 is a photograph in which the shadow of diffraction appears quite clearly, at least in the original, not so well in the reproduction. The partial distribution of the light of the actual image field beyond the angular margin is evident, whereas a dark shadow runs into the image field from the edge.

The shadow of diffraction as it emanates from the edges of the objects present in the object space naturally disturbs the distribution of brightness calculated previously in sensitive adjustments. However, this effect can be compensated by taking two pictures with the same arrangement, once with schliere, once without. With the help of the latter, a value ϵ^* is determined for each point with respect to its brightness which is later to be measured in comparison with the standard schliere. This value ϵ^* is derived from the data for the same point on the other photograph. Naturally this correction will have a purpose only if $\epsilon^* \ll \epsilon$.

Diffraction furnishes a natural limit to the increase of sensitivity. The position of this limit depends upon the exactitude of measurement required, as always. To give generally valid numerical data at this point is

impossible because it has not been possible heretofore to comprehend the nature of the shadow of diffraction theoretically. Consequently, it cannot be stated whether the limit of measurement imposed by diffraction will still be extended by some means or other.

2. COMPARISON OF THE SCHLIEREN METHOD WITH THE MACH-ZEHNDER INTERFEROMETER

In this connection, the question arises whether the schlieren arrangement or the Mach-Zehnder interferometer used to investigate the same problems is more sensitive. A generally valid answer cannot be given since the two methods operate differently.

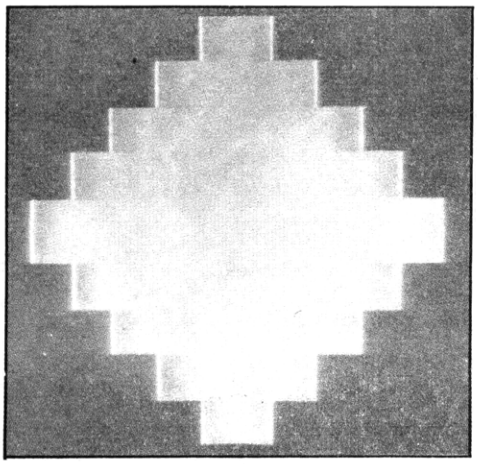

Figure 47 - Result of Diffraction along Schlieren Stop

Brightening occurs along the perpendicular edges beyond the optical field, whereas darkening takes place within the optical field.

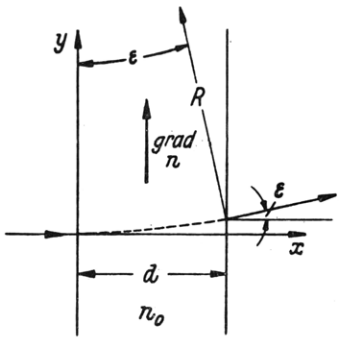

Figure 48 - Light Deflection of Plane-Parallel Plate with Variable Index of Refraction

Basically, the interferometer measures the index of refraction directly, whereas in the schlieren method the deflection depends upon grad n.

As an example, let us take a plane-parallel plate whose thickness is d, Figure 48, and whose index of refraction varies in the y-direction while it remains constant in the x-direction. This plate produces a band deflection of

$$\omega = \frac{d}{\lambda_0}(n - n_0) \qquad [58]$$

in the interferometer.† In the foregoing equation, ω is the band deflection measured in the distance between the bands, n is the variable index of refraction in the plate, n_0 is the index of refraction at one end, and λ_0 is the wave length of the light in a vacuum. Therefore

† H. Schardin, Zeitschrift für Instrumentenkunde, Vol. 53, 1933, pp. 396-424.

$$n - n_0 = \frac{\lambda_0}{d}\omega \qquad [58a]$$

The schlieren method measures the deflection ϵ produced by the curvature of the light ray. This is strongly exaggerated in Figure 48. According to Equation [24], the radius of curvature is $R = \frac{n}{\text{grad } n \sin \varphi}$. When $\sin \varphi = 1$ and $R = d/\epsilon$,

$$\epsilon = \frac{d}{n}\,\text{grad}\, n \qquad [59]$$

This expression corresponds to Equation [58]. Consequently,

$$\text{grad}\, n = \frac{n}{d}\epsilon \qquad [59a]$$

Since the change of n is small, n_0 can be written instead of n on the right side. Then

$$n - n_0 = \frac{n_0}{d}\int \varepsilon_y\, dy \qquad [60]$$

Therefore according to Equation [58a], n is determined directly from the deflection of the band, whereas according to Equation [60], n is to be determined from the integral of the deflection ϵ over y.

This is the basis of the differences between the two methods, and the more suitable method must be chosen according to the requirements of each case. In this respect, see page 65 also.

3. COMPARISON OF TOEPLER'S SCHLIEREN METHOD WITH THE PURE SHADOW METHOD

The direct shadow method, first described by Dvorak in 1880, operates by transmitting light directly through the schliere from a point source of light without any lens. The light source used was as nearly punctiform as possible to attain. This produces a nonuniform distribution of brightness on a white screen which collects the light, as a result of the light refraction in the schliere. This irregular distribution of brightness permits the presence of schliere to be recognized. Figure 49 shows a flow of ether vapor from an open flask, photographed by the shadow method. The light which is deflected by the schliere is not re-united at the same corresponding point in the shadow image from which it emanates in the schliere, as is true in Toepler's schlieren method, but produces some type of distribution of brightness on the screen. This can be clearly recognized in Figure 49, for example, where the vapor emanates from the neck of the flask.

Conditions in the object cannot be calculated from a schlieren photograph made by the shadow method because it cannot be directly established

from which point in the schliere the light reaches a given point on the ground glass, as it can from a schlieren photograph made by Toepler's method. However, if the light is allowed to pass only through definite points in the phenomenon by stopping down, the magnitude of the angles of deflection ϵ for the given points in the phenomenon can be determined after the positions of the corresponding points of light on the ground glass have been established. This method was followed by E. Schmidt to calculate heat transmission in a heated horizontal tube.†

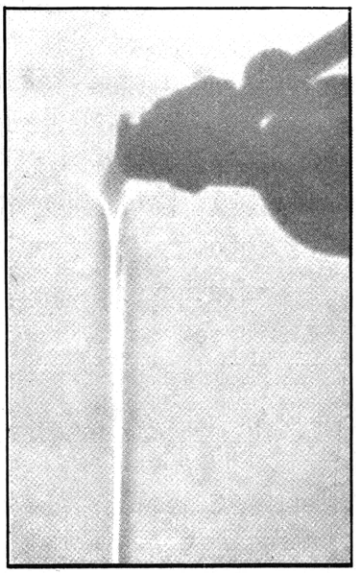

Figure 49 - Ether Vapor Flowing from an Open Flask Photographed by the Pure Shadow Method

From "Heizung und Lüftung" (Heating and Ventilation), December 1932.

The great advantage of the direct shadow method is the extreme simplicity of the arrangement which requires no lens system whatsoever, and which correspondingly permits investigation of phenomena of any given size. Toepler's method requires a rather large supply of optical apparatus. However, in compensation, its advantages compared to the shadow method are:

1. Considerably greater sensitivity. A deflection of the light on the schlieren stop by fractions of a millimeter produces a perceptible variation of brightness, whereas at least one or more millimeters of deflection on the intercepting screen are needed in the shadow method to permit recognition of the shape of the schliere or to allow measurement of the deflection with some accuracy.

2. Photographs taken by the Toepler method are unambiguous. The brightness at a given point on the photograph is determined by the angle of deflection at the corresponding point in the phenomenon. Hence photographs taken by this method permit a reliable impression of the phenomenon without additional efforts of evaluation. Quantitative evaluation of the pure shadow method requires probing the phenomenon with the help of stops. Owing to diffraction phenomena, these stops cannot be made as small as desired.

---

† E. Schmidt, Forschung auf dem Gebiete des Ingenieurwesens, Vol. 3, 1932, p. 181.

3. The object which is to be studied can be photographed reduced. This permits photographing nonstationary phenomena. Since the method deals with transmitted light, the brightness is even sufficient to take slow motion pictures at high image frequency.†

V. EXPERIMENTAL DEVELOPMENT AND CONSTRUCTION

1. CONSTRUCTION OF EXPERIMENTAL APPARATUS

Satisfactory operation of Toepler's schlieren apparatus is possible only if it is set up in a room as shockproof as possible. Operation of large machines cannot be permitted in the vicinity of the apparatus. Moreover, the building must be sufficiently distant from railroads and heavy vehicular traffic. Even shocks produced by walking about in the room are unpleasantly evident. Adjustment of the schlieren stop also depends upon the position which a person takes in the room, because the load exerted on the floor by a human being produces perceptible bending.

It is obvious that the necessary tables, benches, stands, etc., must be very solid. The mounting of the schlieren stop must be especially shockproof.

In a sensitive adjustment, the convection of air present in every room is clearly evident, especially if heating systems are operating or if drafts are present. Therefore, under certain conditions it is necessary to enclose the entire optical path.

If concave mirrors silvered on their front surfaces are used as objectives, they cannot be lacquered, for the coating of lacquer produces strongly disturbing deflections; see Figure 43 which was made with a lacquered mirror. Unfortunately, the absence of lacquer shortens the life of the silver coating of the reflector. In time the surface of the mirror assumes a brown color produced by oxidation. Naturally, when this occurs, a satisfactory quantitative evaluation based on brightnesses is no longer possible.

Light reflections, produced by reflection from the surfaces at the lens O which produce errors in the distribution of brightness in the image field are to be avoided. This can be accomplished by setting the lens obliquely.

---

† Translator's Note: See "Neue Ergebnisse der Funkenkinematographie" (Recent Results in Spark Cinematography), by H. Schardin and W. Struth, Berlin-Gatow, in Zeitschrift für technische Physik, Vol. 18, No. 11, November 1937, pp. 474-477; TMB Translation 107, December 1942.

2. LIGHT SOURCES

In general an arc lamp controlled by clockwork will be used as a light source. Electrically regulated arc lamps are not as satisfactory, for the position of the carbon electrodes changes by mutations. Tungsten arc lamps are also quite usable.

If monochromatic light is desirable, the sodium-vapor lamp fabricated by the Osram Company is recommended.

If the phenomenon is to be photographed, a photographic plate is inserted instead of the ground glass and exposure is made with an instantaneous shutter as long as the rate of change in the phenomenon permits. This instantaneous photographic shutter is usually fabricated as a unit together with the lens O. The free aperture of this shutter, however, must be large enough to admit all deflected rays. It must be noted that an error in the values for brightness may be produced by the shutter. This may be due to the fact, for example, that the shutter permits passage of light rays of greater deflection for a short time only. In such a case the absolute evaluation of brightness might be difficult or tedious. However, the results obtained by comparing the photograph with the standard schliere are almost errorless if the shutter is located in the immediate vicinity of the schlieren stop. Stopping down the light source slit would be more favorable, but would necessitate elimination of scattered light.

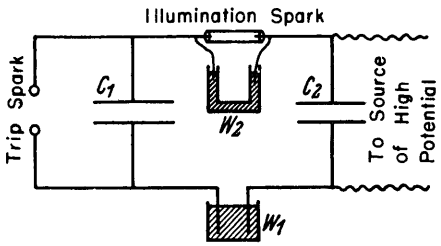

Figure 50 - Mach's Hook-Up

C_1 and C_2 Capacitors
W_1 Damping resistance
W_2 High ohmic resistance

For very high-speed phenomena, pure mechanical control of illumination is no longer possible.† Then electric sparks are used as a light source. The apparatus which permits sparks of maximum brilliance and minimum duration has been reported elsewhere.††

Mach's hook-up, shown in Figure 50, is used to produce illuminating sparks. The two capacitors, C_1 and C_2, of 0.0222 μf each, are charged by a high-voltage motor generator set to about 30-50 kilovolts. The high ohmic water resistance W_2 serves as a conductor for charging C_1. The voltage is

---

† See "Kinotechnik," by H. Schardin, Vol. 14, 1932, p. 41.

†† See "Methoden der Momentphotographie" (Methods of Instantaneous Photography), by Bruno Glatzel, Braunschweig, 1915; "Messung der Funkenhelligkeit und Funkendauer" (Measurement of the Luminosity and Duration of Electric Sparks), by Kornetzki, Fomin, and Steinitz, Zeitschrift für technische Physik, Vol. 14, No. 7, 1933, pp. 274-280, TMB Translation to be published; "Lehrbuch der Ballistik" (Textbook of Ballistics), by C. Cranz, Vol. 3, Berlin, 1927.

measured advantageously by a Starke-Schröder voltmeter. Some arrangement is devised by which the phenomenon to be photographed itself releases the trip spark. This causes breakdown of capacitor C_1, and directly thereafter the illuminating spark jumps. The resistance W_1, which is approximately 10 ohms, serves to damp the illuminating spark circuit aperiodically. Moreover, it must be designed to satisfy given conditions. Brilliance increases greatly with the length of the spark gap. However, the length of the gap is limited by the magnitude of the charge voltage. Figure 51 shows a few photographs wherein the length of the illumination spark gap was varied at constant charging voltage.

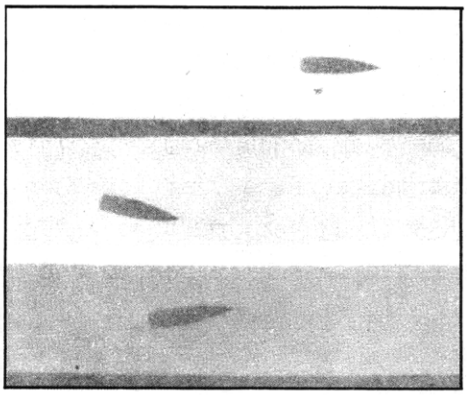

Figure 51 - Spark Photographs of a Flying Projectile Taken by Means of Mach's Hook-Up

The length of the illumination spark gap was varied, whereas other conditions remained constant.

Moreover, to produce a bright and short illuminating spark, precautions must be taken to keep the inductivity of the circuit small. For this reason, the shortest possible leads from the capacitors C_1 and C_2 to the illuminating spark and also to the resistance W_1 should be used.

When using electric sparks as a light source, the grid-screen method described in Part III, page 32, is easy to apply.

Quantitative evaluation of a schlieren photograph by comparison of the values of brightness with those within the standard schliere requires that the image of the light source on the schlieren stop be at least as wide as the maximum deflection. Otherwise, from a given deflection on, the light is completely refracted upward onto the schlieren stop or refracted down from it. The deflection is then no longer determined unambiguously by the brightness.

This requirement cannot be satisfied very easily with electric sparks. It is advantageous to have the spark gap in a thin glass tube to fix the path of the spark to some extent. The inner wall of the glass tube becomes roughened after a short time, due to chemical and mechanical effects, and functions as ground glass. However, a decrease of brightness scarcely results, as most of the inner wall can then be considered practically as the illuminating surface. The latter can be magnified about five times by a condensing lens; see pages 22 and 23. If the inside diameter of the glass

tube used is too large, the spark jumps on irregular paths. Adjustment of the schlieren stop then functions differently from one picture to another, which produces irregular images.

3. SCHLIEREN CINEMATOGRAPHY

It is often desirable to run a strip of film for nonstationary phenomena. For this purpose, the gate aperture of a motion-picture camera must be located at the position ordinarily occupied by the ground glass. In consequence of the smallness of the object and its remoteness, the objective lens of a usual moving-picture camera will not suffice because its focal length is too short. To completely cover the gate aperture, lenses with a focal length

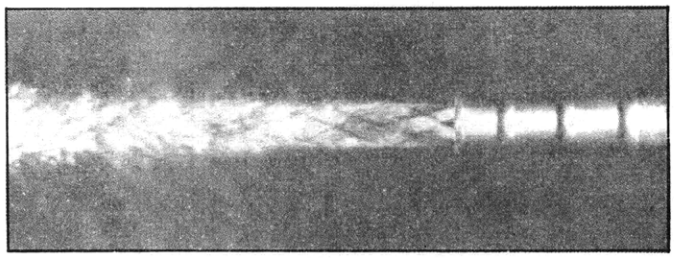

Figure 52 - Schlieren Photograph of Compressed Air Escaping from a Flaring Tubular Nozzle

A spark was used as illumination for the schlieren image, whereas the nozzle itself was illuminated for a few seconds with a nitra-photo lamp.

of about 50 cm (19.68 inches) are necessary. However, it is not requisite that they also have the same speed ratios, for, with the transmitted light from the schlieren arrangement, the brightness is not a function of the aperture ratio at all; see Equation [16]. The diameter of the lens is to be selected only according to the size of the image of the light source and the maximum deflection. However, conditions differ somewhat if a front-light photograph of the objects in the field of view is to be obtained simultaneously with the schlieren image. This is very often desirable, for in this way the schlieren image most generally becomes more comprehensible and clearer, as Figure 52 reveals. For this purpose, the objects must be illuminated obliquely from the front with nitra-photo lamps (Nitraphotlampen), or the like. Naturally, the aperture ratio of the lens then becomes the decisive factor. To exploit the aperture ratio most fully, the schlieren stop should be shifted as close as possible to the edge of the lens thus to free almost the entire opening for the time-exposure light.

Ordinarily, mechanical slow-motion machines can also be used for high-speed phenomena. However, at extreme velocities, electric sparks must

generally be used as light sources. Image frequencies from about 1000 to 100,000 per second can be attained by a steady succession of sparks at a speed of 1000 to 100,000 per second at L (Figure 1), and by mounting the film at P on a rotating drum, so that each new image impinges on unexposed film. However, to increase the size of the images which would otherwise be too small at these higher image frequencies, the cone of light is permitted to impinge upon a rotating mirror after traversing the lens O.

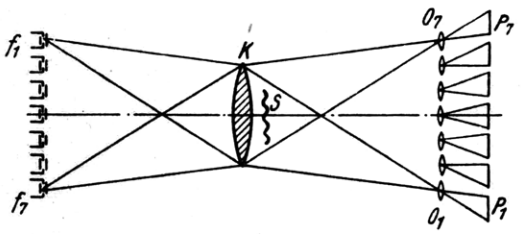

Figure 53 - Basic Arrangement for Motion-Picture Photography at High Image Frequencies on Stationary Film According to Cranz-Schardin

The arrangement shown in Figure 53 permits attainment of maximum image frequencies.† It consists fundamentally of numerous schlieren arrangements with a common objective K. Each spark, f_1 to f_7, jumps only once and, moreover, each jumps at a definite time interval after its predecessor. Thus images are produced on the stationary plates, P_1 to P_7, which corresponds to times separated by the same intervals. This permits attainment of image frequencies up to about 10^7 per second. To be sure, every series of pictures contains only a limited number of individual images, about twenty at the most. In spite of this, these are sufficient to investigate the phenomenon in most cases; see Figure 54.

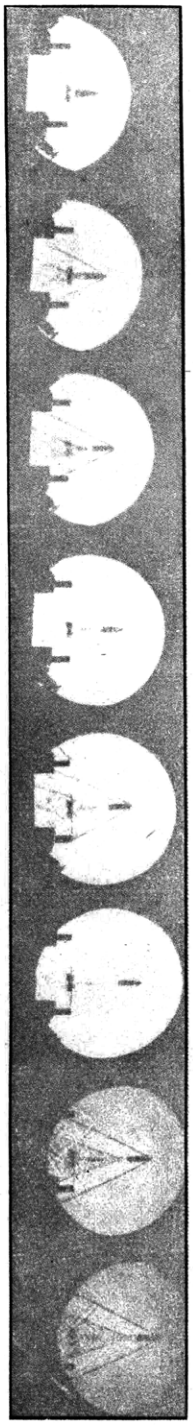

Figure 54 - Strip of Film Showing a Projectile Fired through a Strip of Copper; Image Frequency 100,000 per Second

4. SIMULTANEOUS PHOTOGRAPHY OF LIGHT DEFLECTION IN TWO MUTUALLY PERPENDICULAR DIRECTIONS

On the basis of ideas expressed in Part II, the condition within the schliere is already determined, if only the image for one direction of deflection, i.e., ϵ_y or ϵ_z, is present; for example, provided that the schliere lies entirely in

† C. Cranz and H. Schardin, Zeitschrift für Physik, Vol. 56, 1929, p. 147.

the optical field and that the condition beyond its limits is known. Moreover, the change of state within the schliere must proceed at a constant rate. In spite of this fact, it is often advantageous for interpretation if two pictures of the same phenomenon are taken simultaneously in two directions perpendicular to each other.

This was accomplished practically by transmitting the light from the light source L onto two mirrors S_1 and S_2. These mirrors were totally reflecting prisms. The reflecting faces of these mirrors were slightly inclined with respect to each other; see Figure 55. Thus two images L_1' and L_2' of the light source are produced. For example, the horizontal knife edge

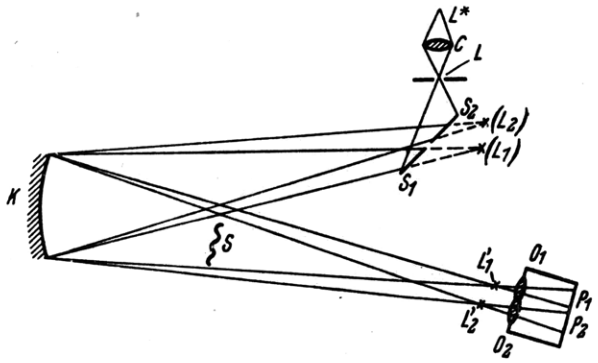

Figure 55 - Arrangement for Simultaneous Photography of Light Deflection in Two Mutually Perpendicular Directions

now functions at L_1' and the vertical one at L_2'. As a result of the astigmatic image differential, one of the two knife edges is set somewhat beyond the other. This is very advantageous from the standpoint of mechanical structure. Now, to get pictures on the plate or film which lie directly alongside each other, two lenses O_1 and O_2 must be used. The distance between the axes of these lenses must be approximately equal to the distance between the midpoints of the images. Furthermore, since the lenses must be of sufficient diameter to collect all deflected rays, it is advantageous to cut off one edge of each lens straight. This is done so that they may be placed against each other closely. Figure 56 is a section from a strip of film showing the convection currents about an incandescent lamp. In the left-hand

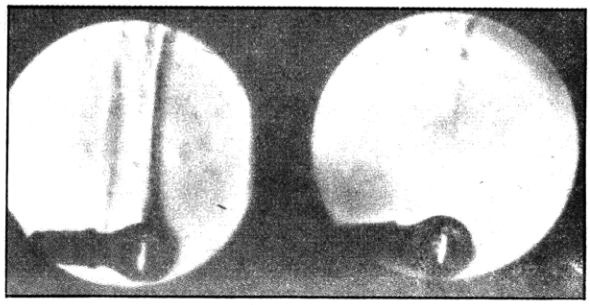

Figure 56 - Heated Air Rising from an Incandescent Lamp

For the left-hand picture the knife edge was vertical; for the right-hand picture it was horizontal.

picture, deflection is horizontal; whereas, in the right-hand one, it is vertical. When the upward flow is exactly vertical, almost nothing can be seen on the right-hand image. However, as asymmetries develop which are mostly related to the scaling-off of vortices, they are particularly pronounced on the right-hand picture of the image. Hence it could be stated in general that the left-hand picture shows the stationary phenomenon, the right-hand picture, in contrast, shows the dynamic phenomena, especially turbulence.

VI. THE APPLICATIONS OF TOEPLER'S SCHLIEREN METHOD

1. GENERAL INFORMATION

The schlieren method may be applied for two reasons:

a. It permits the presence of striations or flaws to be ascertained and furnishes data respecting their external shape. Formerly this was its only application.

b. In the present study it has been proved that quantitative data concerning the condition within the schliere can be obtained. The schlieren method may also be applied for this reason.

2. INVESTIGATION OF TRANSPARENT SOLIDS

The schlieren method is an excellent aid for testing lenses and concave mirrors for flaws. It was used for this purpose especially by Foucault in 1858. For this reason it is also known in practical optics as Foucault's knife-edge test. Discovery of errors in reproduction with the aid of the schlieren method has already been treated in Part I, Sections 5 and 6.

Plane-parallel glass plates can also be investigated. For this purpose an arrangement is used which provides parallel light. If the surfaces are nonparallel, it becomes evident by the fact that the schlieren image of the plate becomes alternately light and dark when rotated. This is known as wedge error. However, at every instant the brightness of the entire surface is uniform. If the surface is not exactly plane, i.e., if it has a definite radius of curvature, one side is brighter than the other, independent of the position of the plate. This is termed the spherical error. Zone errors become evident in a similar way. Nonuniform irregularities of the surface produce a distribution of brightness in the schlieren image which is a function of the position of the plate; see Figure 57.

Figure 58 is the schlieren photograph of a glass plate such as is used for photographic plates. The great unevenness of its surfaces can be

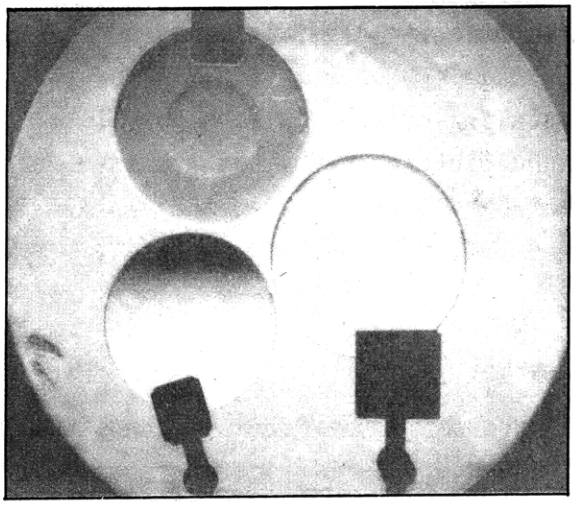

Figure 57 - Investigation of Glass Plates by the Schlieren Method

Upper Plate, Zone Error; Plate at Lower Left, Spherical Error; Right-Hand Plate, Satisfactory.

recognized. Figure 59 shows the schlieren image of a Cellon† plate. The rolling nature of the surface is clearly visible.

The index of refraction of small pieces of glass can be determined by placing them in a mixture of two different liquids whose index of refraction may be varied continuously, owing to the ratio of mixing. The mixture of liquids is put into a cuvette with plane-parallel walls. The fragments of glass can be clearly recognized in the schlieren image as long as the index of refraction of the liquid is not equal to that of the pieces of glass. The

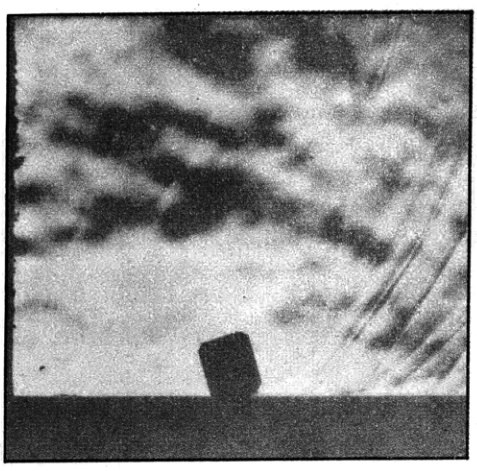

Figure 58 - Striae in a Glass Plate

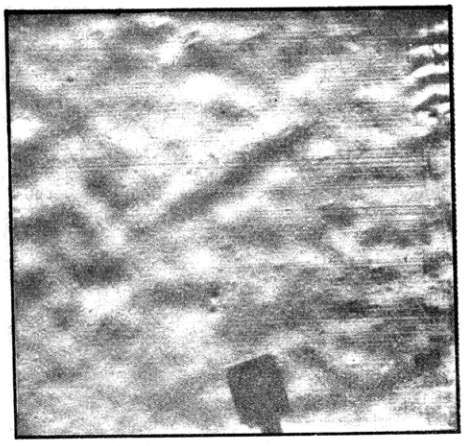

Figure 59 - Schlieren Photograph of a Cellon Plate

† Translator's Note: Cellon is acetylcellulose, a plastic similar to cellophane (cellulose).

schlieren method gives an exact index for the apparent disappearance of the fragments of glass at the instant when the indexes of refraction of liquid and glass coincide. The index of refraction can then be determined directly from the mixing ratio of the two liquids with the aid of a calibration chart.†

It should be possible to apply the schlieren method similarly to clearly ascertain precipitations otherwise very difficult to perceive.

3. INVESTIGATION OF PHENOMENA IN LIQUIDS

With the help of the schlieren method, the following phenomena in liquids can be investigated:

Changes in concentration or density within the liquid as produced by thermal effects. Temperature variations are also occasioned, among other factors, by thermolysis accompanying vaporization of the liquid.

The phenomenon of heat convection which occurs when heating pipes traverse water, as important in engineering, for example.

Phenomena of diffusion. Determination of diffusion constants was already achieved by the pure shadow method in 1893 by O. Wiener.†† On the basis of present observation, Toepler's schlieren method can be applied for the same purpose. As a result of its greater sensitivity, the present method should yield even more comprehensive results. Rough calculation has shown that the differences in concentration in solutions of highly molecular substances, such as sugar in a revolving cuvette at equilibrium of sedimentation, are sufficient to permit measurement. Therefore, the schlieren method might indirectly furnish a possibility for determining the atomic weight of such substances.

Variations in concentration produced by the intensity of an electric field in electrolysis.

Compression waves in a liquid. A shock wave in water can be produced by an electric spark jumping below the surface. This wave can be made visible by the schlieren method. The purpose of such photographs is the investigation of sonic waves in water, as applied in echo-sounding devices.

If the beam of light of a schlieren apparatus is permitted to be reflected from the surface of a liquid, deflections which are a function of

---

† Among other data, liquids suited to this purpose are enumerated in F. Rinne and M. Berek, "Anleitung zu optischen Untersuchungen mit dem Polarisationsmikroskop" (Introduction to Optical Investigations with the Polarization Microscope), Leipzig, 1934, page 207.

†† O. Wiener, Wiedemann's Annalen der Physik, Vol. 49, 1893, p. 105.

the contour of the surface will be obtained. In this way photographs of the propagation of surface waves can be taken which show very striking contrasts. H. Bénard† was the first to determine experimentally the origin and the principles governing a vortex train.†† He used a water trough floored with a glass plate, and transmitted light from below. He was not conscious of the fact that he was applying the schlieren method in principle, to be sure. A special schlieren stop was unnecessary because the deflections were very large, and the frame of the objective lens functioned as a stop.

4. INVESTIGATION OF NORMAL PHENOMENA OF FLOW IN GASES

The principal field of application of the schlieren method lies in the investigation of phenomena in gases. These present great difficulties to the techniques of measurement in physics, such as the investigation of the phenomena of flow in gases. The insertion of probes often disturbs the normal phenomenon in an uncontrollable way. Moreover, an impression of the entire phenomenon can be formed only after a number of individual measurements. If the phenomenon is nonstationary this method cannot be used.

If temperature is to be measured, a thermo-element is inserted at the point where it is required. However, the latter again disturbs the thermal distribution.‡ To investigate the course of flow, smoke is often admixed with the gas. However, the smoke particles will not always describe the same streamlines as the gas particles as a result of their inertia.

The application of the schlieren method to the study of normal phenomena of flow in gases is certainly not very simple, i.e., phenomena which occur at moderately high speeds and in which changes in gas temperature due to heat-releasing bodies are precluded. This is due to the fact that the attendant variations in concentration are generally too small to produce sufficient deflection of light, in spite of the fact that air is considered incompressible up to flow velocities of 100 m/sec (328.08 feet per second) in aerodynamic theory, for example. In this respect compare Table 4.

Therefore, to render air streamlines visible, a variation in density or concentration must be produced artificially. This is most simply accomplished by heating the air somewhat where the streamlines are to be made visible. L. Mach ‡‡ has already used this method. He used the arrangement

---

† H. Bénard, Comptes Rendus de l'Académie des Sciences, Paris, 1908, Vols. 146 and 147, p. 970.

†† These vortex trains were later treated theoretically by von Kármán.

‡ Compare K. Jodlbauer, Forschung auf dem Gebiete des Ingenieurwesens, Vol. 4, 1933, p. 157.

‡‡ L. Mach, Zeitschrift für Luftschiffahrt und Physik der Atmosphäre, 1896, p. 129.

TABLE 4

Index of Refraction n as a Function of Temperature, Pressure, Density, and Velocity of Flow for Variation of Adiabatic Condition

Index of Refraction n	Temperature degrees C p = Const = 760 mm	Pressure mm of Hg t = Const = 0 degrees C	Variation of Density per cent of the Density at 0 degrees C	Velocity m/sec
1.000292	0	760.0	0.000	0.0
1.000291	1	757.4	0.354	27.2
1.000290	2	754.5	0.708	39.8
1.000289	3	751.7	1.062	48.7
1.000288	4	749.0	1.416	56.3
1.000287	5	746.5	1.77	62.9
1.000286	6	743.6	2.13	68.9
1.000285	7	741.1	2.48	74.7
1.000284	8	738.3	2.83	79.8
1.000283	9	735.7	3.18	84.6
1.000282	10	733.1	3.54	88.3

shown in Figure 60 where K_1 and K_2 are the two halves of an achromatic lens having an aperture of 23 cm (9.05 inches) and a focal length of 3 m (9.84 feet). Together, these two lenses form the schlieren objective; furthermore, they form part of the walls of a duct of flow R. A propeller P draws air through the duct from Q; this air is nonuniformly heated by a burner situated at Q. To prevent transmission of propeller vibrations to the schlieren objective, a joint fabricated of tracing cloth is inserted into the duct at W. The phenomenon to be examined takes place between K_1 and K_2. Since the air sucked by the propeller is not uniformly heated and since Mach had provided no modulators, the flow was somewhat turbulent. No regular streamlines can be seen in the schlieren image. Therefore, to get an impression of the dynamic phenomenon on a photographic plate, exposure must be prolonged slightly. This produces a certain lack of sharpness which results from this motion. The very same method is used for taking the well-known photographs of flow obtained by scattering powdered aluminum and lycopodium powder on the surface of water.†

† Compare L. Prandtl and O. Tietjens, "Hydro- und Aeromechanik" (Hydromechanics and Aeromechanics), Vol. 2, Springer, Berlin, 1931.

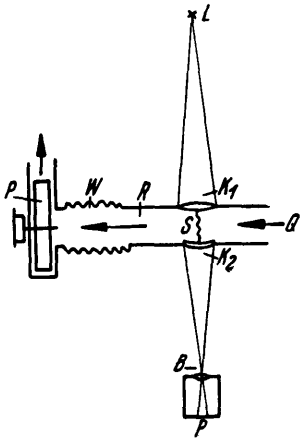

Figure 60 - Mach's Arrangement to Make Streamlines in Air Visible

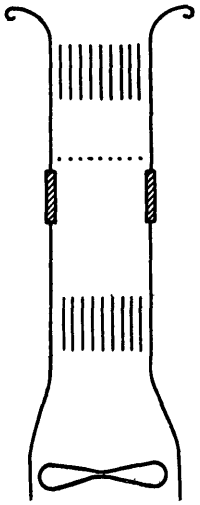

Figure 61 - Flow Duct to Make Streamlines in Air Visible

Attempts were made to improve Mach's apparatus. The new flow duct was sealed by two plane-parallel glass plates. Furthermore, flow modulators were built into the duct and the intake was designed to prevent the formation of turbulent flow as far as possible; see Figure 61. The air was heated by arranging thin electric heating elements at regular intervals in the duct directly in front of the object to be investigated. This permitted favorable regulation of temperature. With this apparatus, flow pictures were taken which reproduced the streamlines regularly and uniformly. They are almost as admirable as those obtained with Pohl's flow apparatus. Figures 62 to 65 are photographs taken with the improved wind tunnel just described. The photographs show the streamlines produced by a compressed air injector sucking in air from the outside.†

Phenomena of flow can be made visible also by admixture of a second gas. Since the deflection of light depends only on the index of refraction, it would be desirable to have a gas possessing approximately the same density and viscosity as air, but whose index of refraction differs from it as greatly as possible. Then the second gas would in no way disturb the pattern of flow. Table 5 shows the characteristic values for several gases.

It can be seen that acetylene is especially suitable as an auxiliary gas. However, the danger of explosion is a deterrent factor. Perhaps the admixture of other inert gases might produce a more suitable combination.

---

† Kölliker, Chemische Fabrik, Vol. 6, 1933, p. 299.

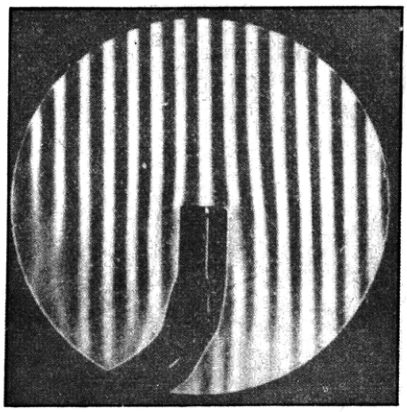

Figure 62

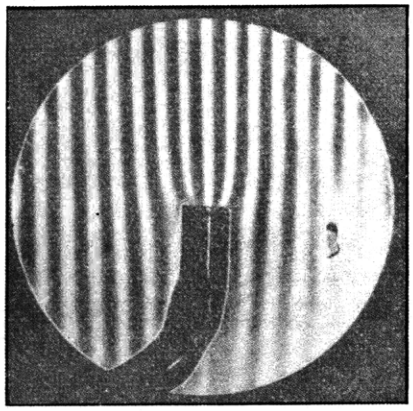

Figure 63

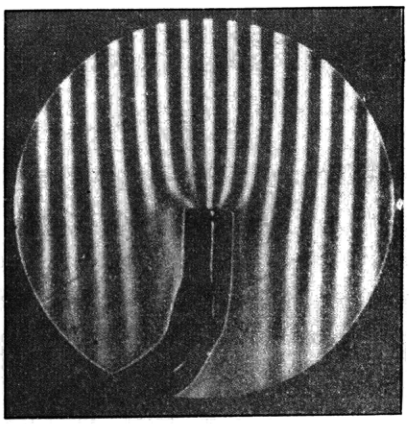

Figure 64

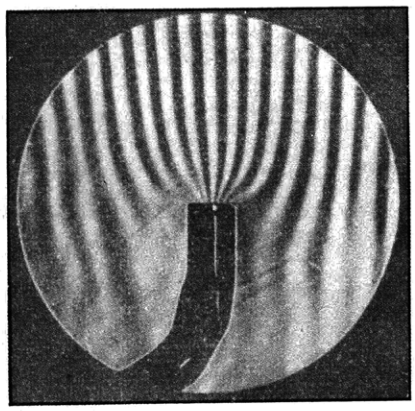

Figure 65

Figures 62 to 65 - Airflow Made Visible

Air, flowing downward at 1.5 meters per second (4.92 feet per second), was drawn from a wind tunnel by means of compressed air injectors at rates of 0, 50, 100, or 300 liters per minute (0, 1.76, 3.53, or 10.54 cubic feet per minute).

Some time ago a series of tests on labyrinth stuffing boxes of steam turbines were made by the author for the Allgemeine Elektricitäts-Gesellschaft (General Electric Company of Germany). In these tests, carbon dioxide was used as an auxiliary gas to make the flow visible. Figure 66 is a photograph of the flow in one chamber of the labyrinth stuffing box.

Ether vapor was used by Wachsmuth† to make the flow of air from a pipe visible. As publications by Wachsmuth and his students show, the schlieren method is also well suited for investigating tone production in wind instruments. Further applications in acoustics will be discussed in Part VI, Section 7.

---

† See references to Wachsmuth and Klug in the bibliography, pages 78 and 82.

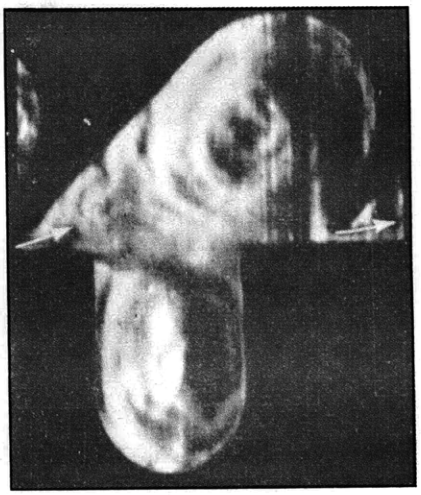

Figure 66 - Model Test on the Vortex Formation in a Chamber of a Labyrinth Stuffing Box

The flow was made visible by mixture of carbonic-acid gas and air. The arrows indicate the place and direction of intake and exhaust flow.

TABLE 5

Characteristic Numbers of Gases

Gas	Index of Refraction n_0 for the D-Line	Specific Weight γ for 0 degrees C 760 mm of Hg kg/m^3	Absolute Viscosity $10^6\ \eta$ $kg\text{-}sec/m^2$
Air	1.000292	1.293	1.750
Oxygen	1.000272	1.429	1.920
Nitrogen	1.000296	1.251	1.680
Hydrogen	1.000143	0.090	0.840
Ammonia	1.000373	0.771	0.950
Carbon Monoxide	1.000335	1.250	1.670
Carbon Dioxide	1.000449	1.977	1.400
Methane	1.000444	0.717	1.040
Acetylene	1.000510	1.179	0.943

5. INVESTIGATION OF THE RECIPROCAL BEHAVIOR OF TWO GASES

In the foregoing discussion, the second gas served only as an auxiliary agent. Here, however, phenomena will be discussed in which study of the behavior of two gases with respect to each other was the experimental object.

In classroom instruction it is often proved that, as a result of its high specific weight, carbon dioxide behaves as a liquid and can be

Figure 67 - Pouring Carbon Dioxide out of an Erlmeyer Flask

With direct illumination, a tone photograph of the objects is obtained simultaneously.

poured from one vessel into another. The proof is supplied by a candle which necessarily must be extinguished in carbon dioxide. With the help of the schlieren method, pouring of carbon dioxide can be made directly visible very easily, as seen in Figure 67.† Under certain conditions, the schlieren method also can be applied to the study of the spread or propagation of poison gases; for example, to test gas masks. As a consequence of the very small optical fields, it is unfortunately impossible to pursue larger clouds of poison gas as they drift. However, photographs on a model scale could be produced for an educational film.

6. HIGH-SPEED FLOW

For velocities of flow in the range of sonic speeds, the variations in density are adequate to produce sufficient deflections of light. Therefore investigations of phenomena in the field of dynamics of gases constitute a principal field of application of the schlieren method. Figure 68 is a photograph of the flow from a nozzle at supersonic speed.††

The movement of air about a flying projectile also belongs in the category of flow at supersonic speed. The first schlieren photographs of a projectile were made by E. Mach. He also gave the correct explanation for the head wave of the projectile. The so-called Mach angle was named for him,

Even purely qualitative observation of schlieren photographs of a projectile furnish a key to the nature of the resistance of projectiles. Furthermore, by measurement of the angles of the head and tail waves, they supply a possibility for measurement of the speed of the projectile.

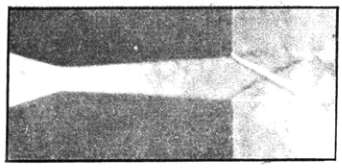

Figure 68 - Flow of Air at Supersonic Velocity from a Rectangular Nozzle

The quantitative evaluation of schlieren photographs herein described should augment their value considerably. Producing

† A series of such and similar photographs were made by the author for the educational film "Unsichtbare Wolken" (Invisible Clouds), for the UFA Motion Picture Corporation.

†† See J. Ackeret, "Gasdynamik" (Dynamics of Gases), Handbuch der Physik, H. Geiger and K. Scheel, Vol. 7, Springer, Berlin, 1927.

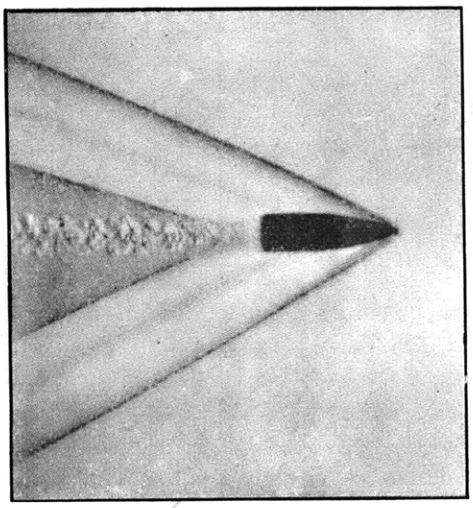

Figure 69 - Schlieren Photograph of a Projectile Traveling at 900 Meters per Second (2950 Feet per Second)

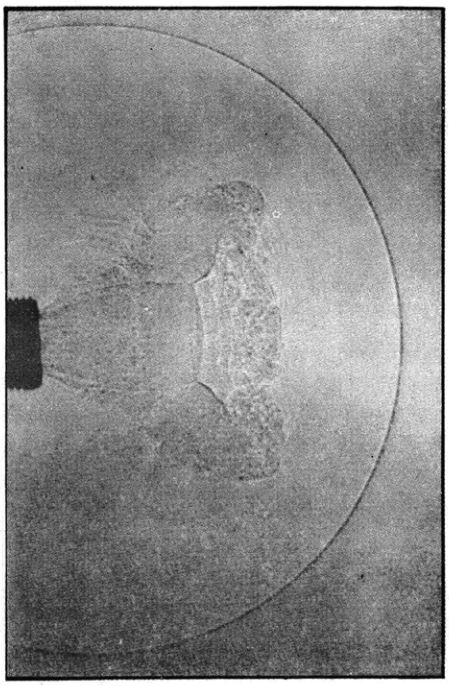

Figure 70 - Flow of Air from a Gun Barrel on the Firing of a Projectile

The projectile is still in the barrel.

a schlieren photograph is considerably simpler than producing an interference photograph capable of evaluation. The reasons are as follows: A larger optical field is available in schlieren photography, the use of monochromatic light is unnecessary, and, finally, the painstaking and time-consuming adjustment of the interferometer is obviated. Figure 69 is a good schlieren photograph of a flying projectile.

Moreover, the phenomena at the muzzles of weapons at the exit of projectiles can be followed and measured. In part, they correspond very closely to normal flow from nozzles. At this point, reference to Figures 70, 71, and 72 should suffice.

Flow at supersonic speeds plays a part in other fields of engineering also; for example:

1. Flow from jets in steam-turbine engineering.†

2. In the theory of autogenous (oxygen) cutting or welding torches, the flow from nozzles is a decisive factor also.††

---

† A. Stodola, "Dampf- und Gasturbine" (Steam and Gas Turbines), Vol. 6, Springer, Berlin, 1924.

†† See H. Malz, "Die Grenzen der Schneidegeschwindigkeit beim Brennschneiden" (The Limits of Cutting Speeds for Cutting Torches), Dissertation der Technischen Hochschule, Berlin, 1932.

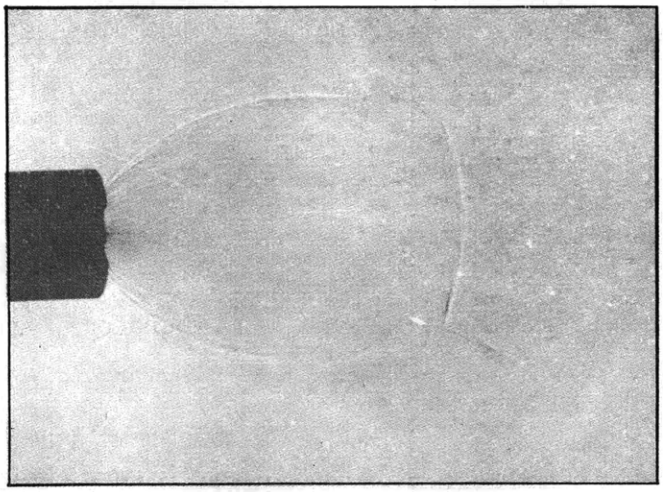

Figure 71 - Flow of the Powder Gases from the Gun Barrel After the Projectile Has Left the Muzzle

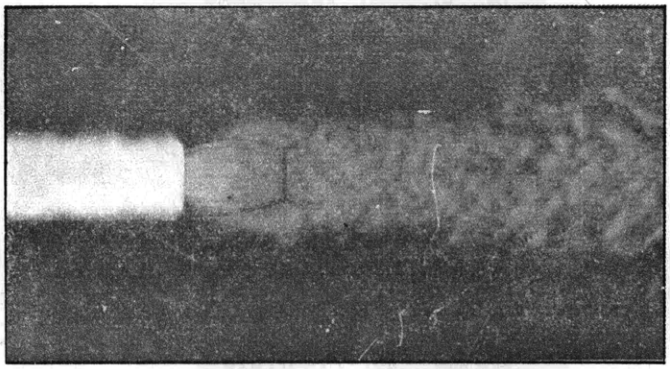

Figure 72 - Steady Flow of Compressed Air from a Cylindrical Nozzle

Compare this photograph with Figures 70 and 71.
[Figures 69 to 72 were taken from Deutsche Jäger-Zeitung Vol. 100, No. 22, 1932.]

3. Blade tips of high-speed propellers move at velocities within the range of sonic speed. A few studies on this subject have already been made.†

7. INVESTIGATION OF ACOUSTIC PHENOMENA

The sound which we perceive with our ears is a vibratory phenomenon in the surrounding air. The variation in the condition of the air can be assumed as adiabatic. The problem will now be considered whether, at the density variations occurring in practice, the sensitivity of the schlieren method is sufficient to make the sound waves visible.

---

† These studies were made in the Aeronautical Institute at the University of Tokyo.

For this purpose a plane sonic wave will be assumed which is produced by a vibrating diaphragm. The equation of motion of the diaphragm is

$$x = A \sin 2\pi\nu t \qquad [61]$$

where x is the displacement,
t is the time,
A is the amplitude, and
ν is the frequency.

The velocity u of the diaphragm and, therefore, that of the air situated directly in front of it is expressed

$$dx/dt = u = 2\pi\nu A \cos 2\pi\nu t \qquad [62]$$

Based on the adiabatic equation, a definite pressure of the air situated directly in front of the diaphragm can be ascribed to each velocity,† i.e.,

$$u = 2\pi\nu A \cos 2\pi\nu t = \frac{2a_0}{\varkappa - 1}\left[\left(\frac{p}{p_0}\right)^{\frac{\varkappa-1}{2\varkappa}} - 1\right] \qquad [63]$$

where p is the pressure,
p_0 is the static pressure,
ρ_0 is the static density,
$\kappa = c_p/c_v$,†† and
a_0 is the sonic speed in static air at infinitely small amplitude.

If the ratio of densities ρ/ρ_0 is substituted for the ratio p/p_0, then

$$2\pi\nu A \cos 2\pi\nu t = \frac{2a_0}{\varkappa - 1}\left[\left(\frac{\rho}{\rho_0}\right)^{\frac{\varkappa-1}{2}} - 1\right] \qquad [64]$$

Substituting the ratio of refraction from Equation [25], Equation [65] is obtained:

$$\left.\begin{aligned} 2\pi\nu A \cos 2\pi\nu t &= \frac{2a_0}{\varkappa - 1}\left[\left(\frac{n-1}{n_0-1}\right)^{\frac{\varkappa-1}{2}} - 1\right] \\ \text{or } \frac{n-1}{n_0-1} &= \left[\frac{(\varkappa-1)\pi\nu A \cos 2\pi\nu t}{a_0} + 1\right]^{\frac{2}{\varkappa-1}} \end{aligned}\right\} \qquad [65]$$

---

† See J. Ackeret, "Gasdynamik" (Dynamics of Gases), Handbuch der Physik, H. Geiger and K. Scheel, Vol. 7, Springer, Berlin, 1927, p. 324.

†† c_p is the specific heat of air at constant pressure and c_v is the specific heat of air at constant volume.

Since the expression in brackets of the latter equation differs only by a little from unity, Equation [66] can be written as an approximation:

$$\frac{n-1}{n_0-1}=1+\frac{2\pi\nu A}{a_0}\cos 2\pi\nu t \qquad [66]$$

This equation expresses the variation in the index of refraction directly on the surface of the diaphragm. Correspondingly the spatial distribution of the projected sound must be

$$\left.\begin{aligned}\frac{n-1}{n_0-1}&=1+\frac{2\pi\nu A}{a_0}\cos\frac{2\pi\nu x}{a_0}\\ n&=1+(n_0-1)\left(1+\frac{2\pi\nu A}{a_0}\cos\frac{2\pi\nu x}{a_0}\right)\end{aligned}\right\} \qquad [67]$$

The deflection of light can be calculated with the aid of this equation if parallel light traverses the sonic beam perpendicularly.

According to Equation [59]

$$\varepsilon\approx\frac{d}{n_0}\,\mathrm{grad}\,n,$$

where d is the effective width of the sonic field. Moreover,

$$\mathrm{grad}\,n=\frac{dn}{dx}=(n_0-1)\frac{2\pi\nu A}{a_0}\,\frac{2\pi\nu}{a_0}\cos\frac{2\pi\nu x}{a_0} \qquad [68]$$

$$(\mathrm{grad}\,n)_{\max}=(n_0-1)\left(\frac{2\pi\nu}{a_0}\right)^2 A \qquad [69]$$

$$\varepsilon_{\max}=\frac{d}{n_0}(n_0-1)\left(\frac{2\pi\nu}{a_0}\right)^2 A \qquad [70]$$

To check whether the greatest angle of deflection $\epsilon_{\max}$ is sufficient for a variation of brightness which can be determined, numbers will be substituted. The greater the frequency and amplitude, the greater ϵ becomes. On the basis of considerations of the strength of vibrating diaphragms, Equation [71] can be set as an approximation for maximum amplitude attainable,

$$A_{\max}\,\nu=10 \qquad [71]$$

where $A_{\max}$ is measured in centimeters and ν in cycles per second. The value $\epsilon = 10^{-5}$ can still be ascertained. For example, let the width of sonic field d be 5 cm (1.969 inch); moreover $n_0 - 1 = 0.000292$, $a_0 = 34{,}000$ cm/sec (1115 feet per second). It is then found that

$$\varepsilon=5\cdot 0.000292\cdot\frac{4\pi^2\cdot 10}{11.56\cdot 10^8}\,\nu=5\cdot 10^{-10}\,\nu$$

When $\epsilon = 10^{-5}$

$$\nu = 0.2 \cdot 10^5 = 20{,}000 \text{ cycles}$$

This consideration shows that it must be possible to make sound directly visible at great amplitudes and at high frequencies with the aid of the schlieren method. It is to be expected that the quantitative evaluation here given will produce a result which gives a method of recording sonic phenomena oscillographically without disturbing the sonic field by a microphone or the like.†

The supersonic waves produced by a quartz oscillator already have been made visible directly by E.P. Tawil.††

Deflections which far exceed the limit of sensitivity are produced by so-called shock waves. These are sonic waves having a very steep front and great intensity. They are produced by a breakdown spark or by an explosion. The velocity of propagation of such shock waves is a function of the intensity. This is proved by Figure 73, for example, in which two shock waves are visible which emanate from two powerful sparks produced simultaneously. The diameter of the more intensive shock wave exceeds that of the weaker. An application can be found in photographing the sonic waves or shock waves for purposes of room acoustics and structural acoustics. For example, at the location of the sonic source, such as the speakers' platform or the orchestra pit in the model of a hall, a spark gap is placed. The shock waves emanating from it are reflected similarly as in a full-scale hall. In this way the audibility at individual points can be studied. Photographs of this type were taken by Sabine.‡

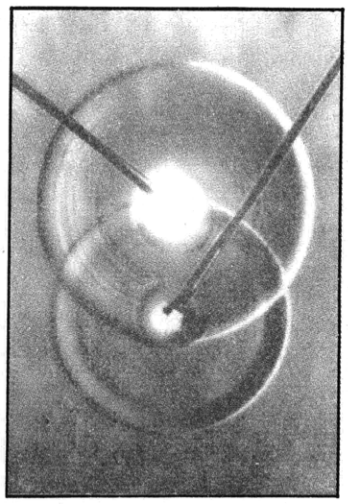

Figure 73 - Schlieren Photograph of Two Shock Waves of Differing Intensities Produced Simultaneously

The overlapping of two shock waves of high intensities is interesting. This superposition is not linear;

---

† Similar experiments were made by A. Raps with the help of the interference refractor. Compare A. Raps' Annalen der Physik und Chemie, Vol. 50, 1893, p. 193.

†† E.P. Tawil, Comptes Rendus de l'Académie des Sciences, Paris, Vol. 191, 1930, p. 92 and 998.

‡ Collected Papers on Acoustics, 2nd Edition, Cambridge, 1923.

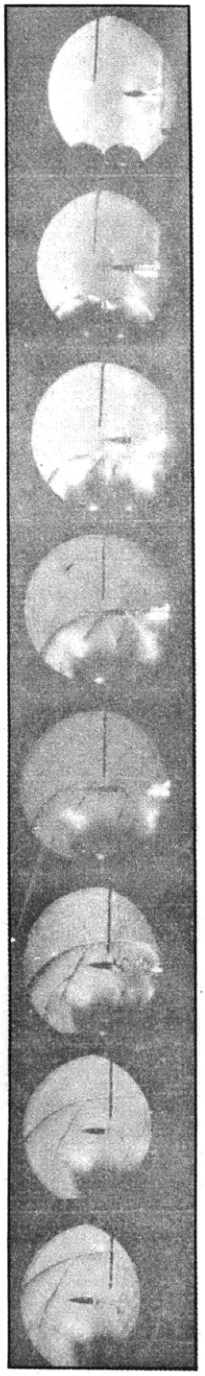

it is subject to more complex principles.† Figure 74 shows such overlapping of two explosive shock waves, produced by firing two small heaps of silver fulminate.

If the schlieren image of the shock wave of an explosion is projected through a slit behind which a moving film is situated, the distance-time curve of the propagation of the wave is obtained. Photographs of this type were taken by Gawthrop.††

8. THERMO-HYDRODYNAMIC PHENOMENA

As can be perceived from Table 4, small temperature variations suffice to produce perceptible deflections ϵ. Thus, for example, Figure 75 shows the heated air rising from a lighted incandescent lamp. Figure 43 showed the warm air produced by exhalation made visible by the schlieren method.

Therefore the schlieren method is well suited for investigating thermo-hydrodynamic phenomena. Moreover its applications can be categorized as follows:

a. The study of the movement of hot or cold air.

b. Quantitative evaluation of the temperature field for which an example was treated in Part III.

In most cases it is unfortunately impossible always to study the thermo-hydrodynamic fields of flow in full scale owing to the limited dimensions of the available mirrors. It is generally necessary to induce full-scale conditions from photographs of models. Therefore

Figure 74 - Motion-Picture Film of the Overlapping of Two Shock Waves Produced by Explosion

The so-called Mach's V-propagation (Mach effect) can be recognized. [From C. Cranz and H. Schardin, Zeitschrift für Physik, Vol. 56, 1929, p. 147.]

---

† H. Schardin, Physikalische Zeitschrift, Vol. 33, 1932, p. 60.

†† D.B. Gawthorp, Review of Scientific Instruments, Vol. 2, 1931, p. 522; ibid., Journal of the Franklin Institute, Vol. 214, 1932, p. 647.

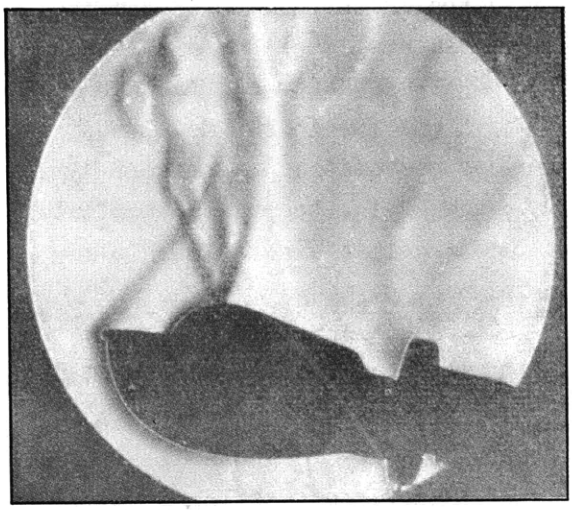

Figure 75 - Heated Air Rising from an Incandescent Lamp

the problem of the scale ratio of model similitude will be taken up here.

If a thermo-hydrodynamic phenomenon is produced by free convection only, the full-scale tests and the model tests are similar if Grashof's coefficient Gr and Stanton's coefficient St are equal for both. That is

$$Gr = \frac{l^3 \varrho^2 \beta (\vartheta_w - \vartheta_\infty) g}{\eta^2} \qquad [72]$$

For gases the following equations are particularly valid

$$Gr = \frac{l^3 \varrho^2 (\vartheta_w - \vartheta_\infty) g}{\eta^2 \vartheta_\infty} \qquad [73]$$

and

$$St = \frac{\lambda}{c_p \eta} \qquad [74]$$

where l is a characteristic length,
ρ is the density,
β is the coefficient of expansion,
ϑ_w is a characteristic wall temperature,
ϑ_∞ is the temperature at a remote distance,
g is the acceleration of gravity,
η is the absolute viscosity,
λ is the capacity for heat conduction, and
c_p is the specific heat.

Fortunately, Stanton's condition is satisfied directly for gases if the problem deals with gases having the same atomic number. Therefore, to attain complete similitude for two experiments, equality of the term Gr for

both is sufficient. If in the investigation of the field of flow, for example in a heated room, the scale ratio of the dimensions of model and prototype is only $1/\alpha$, either the temperature differences in the model must be α^3 times the prototype or the densities in the model must be $\sqrt{\alpha^3}$ times as great, which is produced by varying the static pressure if similitude is to be maintained in the model test. Or again, to prevent too great temperature or pressure differences in the model, the relationship $p'/p = \nu_p$ is selected; then the temperature ratio must be $\nu_\vartheta = \vartheta'/\vartheta = \alpha^3/\nu_p{}^2$.

For example, using a scale ratio of 1 to 5, the following possibilities arise. Either the temperature difference to be produced in the model must be 125 times as great, or the pressure in the model must be 11.2 times as great. Or again, if the pressure in the model is taken only 3 times as great, the temperature differences must be 125/9 = 13.9 times as great.

In the foregoing, it is presumed that the viscosity for model and prototype is equal and, furthermore, that Stanton's conditions remain satisfied. This will not agree exactly, for the coefficients of the materials involved are functions of temperature. To compensate for the variations, the temperature ϑ_∞ at a great distance can be varied in the model test.

Presupposing similitude, mutually corresponding amounts of heat in the prototype (Q) and in the Model (Q') have the following ratio,

$$\frac{Q}{Q'} = \frac{\lambda(\vartheta_w - \vartheta_\infty)l}{\lambda'(\vartheta'_w - \vartheta'_\infty)l'} \qquad [75]$$

where all magnitudes pertaining to the model test are indicated by the prime sign. The expression

$$Nu = \frac{Q}{\lambda(\vartheta_w - \vartheta_\infty)l} \qquad [76]$$

is known as Nusselt's coefficient. A very definite value of Nu pertains to each value of Gr. The function $Nu = f(Gr)$ is the characteristic function which completely defines a problem having similar boundary conditions. To correct the functional relationship of the temperature with respect to the indexes of the material, a new coefficient $Te = \frac{\vartheta_w - \vartheta_\infty}{\vartheta_\infty}$ can be introduced as a new parameter.†

Since problems of heating engineering depend fundamentally on conditions of flow, investigation by the schlieren method should be of great value in conjunction with technical measurements of heat transmission. This method supplies a means of giving the picture of the state of flow corresponding to every value of the characteristic function of a definite boundary

† R. Hermann, Physikalische Zeitschrift, Vol. 33, 1932, p. 425.

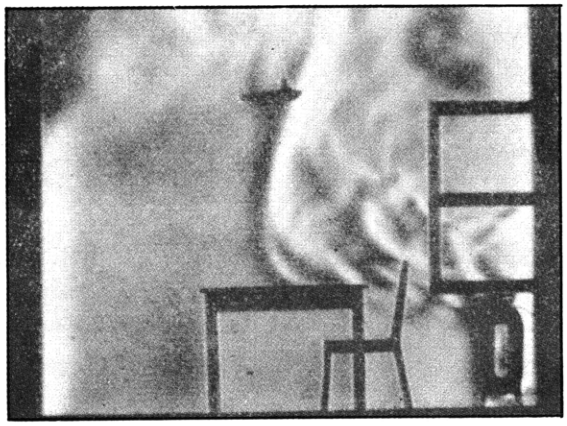

Figure 76 - Model Test on the Flow of Air in a Heated Room on Opening a Window

[From "Heizung und Lüftung" (Heating and Ventilation), December 1932.]

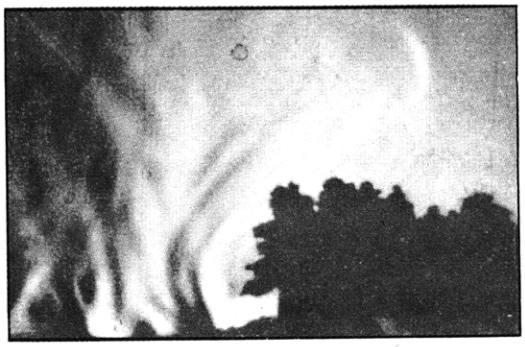

Figure 77 - Heated Air Rising from a Cultivated Field (Model Test)

problem. Furthermore, in simple cases it permits quantitative evaluation of the temperature field. As an example of photographs of models, the flow in a heated model of a room, Figure 76, and a photograph of the heated air rising from a scale model of a cultivated field heated by the sun, Figure 77, are reproduced.

9. DEFORMATION OF REFLECTING SURFACES

Applications of Toepler's schlieren method discussed hitherto were based on light refraction in transparent media. However, the reflection of light can be made useful in a similar manner. If S in Figure 78 is a plane reflecting surface upon which a converging beam of light impinges, whose focal point lies at L', every deviation from the plane state of the surface S will become evident in the schlieren image by insertion of a standard schlieren stop. At the suggestion of Prandtl, this method was used by A. Nadai† to make plastic deformations visible.

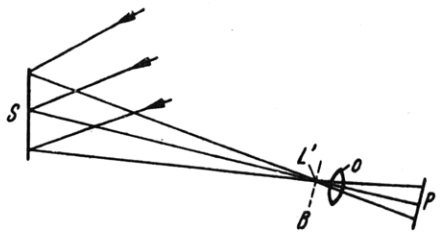

Figure 78 - On the Investigation of the Bending of a Reflecting Surface S

L' - Image of the light source
B - Grid screen
O - Lens
P - Photographic plate

The grid-screen method, described in Part III, can also be advantageously applied here for quantitative evaluation. Figure 79 shows the isophotes for a glass plate 170 mm (6.69 inches) in diameter which was supported

† A. Nadai, Proceedings of the American Society for Testing Materials, Vol. 31, 1931, p. 2.

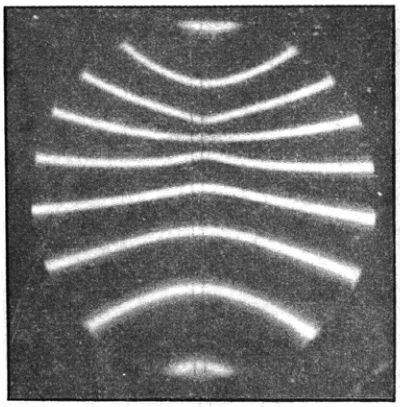

Figure 79 - Isophotes for a Plate Loaded Eccentrically

on its edge and which was bent by about 0.1 mm (0.00394 inch) at a point 25 mm (0.984 inch) from the center. Each isophote is a curve of equal inclination of the plate perpendicular to the direction of the bars of the grid screen. Thus the slope of the surface of the glass plate at every point is known, and by integration the deformation of the surface itself can be derived. This new method can be applied to an experimental treatment of the theory of elasticity, to the theory of the vibration of plates, i.e., the contour of vibration of loud-speaker diaphragms, to measurements of pressure, and to similar phenomena.

10. FURTHER APPLICATIONS

Possible applications of Toepler's schlieren apparatus have not been exhausted with the enumeration of the fields so far considered. Among others, the following additional applications of the method will be mentioned.

In photographing shock waves produced by electric sparks, it was revealed that an intensive movement of the air in the vicinity of the electrodes can be observed even before the spark jumps. This case probably involves photographic recording of the so-called electric wind. After the spark has jumped, the heated air in the gap expands. However, since this air is still electrically charged, it does not flow uniformly in all directions but moves toward one electrode. Closer investigation of this phenomenon should contribute some information to the theory of the electric spark.

Perhaps it may be possible also to measure the variations of density produced in gases produced by "electrostriction."

Toepler has already reproduced the schlieren apparatus in the microscope. These experiments have since been resumed several times but have not culminated in any method which has been adapted to practice as yet. Such a technique, however, should certainly be very useful. Under certain conditions fine details in the object are visible which otherwise can be recognized only after the preparation has been dyed.

BIBLIOGRAPHY

In addition to Toepler's own publications, contributions to Toepler's schlieren method itself are restricted to a few short treatises only, which, however, do not essentially transcend the information already

stated by Toepler. Therefore, as far as possible, the following bibliography includes all studies which are in any way related to the schlieren method. The arrangement is chronological.

(1) "Mémoire sur la construction des télescopes en verre argenté" (A Treatise on the Construction of Telescopes with Silvered Glass), by Léon Foucault, Annales de l'Observatoire Impérial de Paris, Vol. 5, 1859, pp. 197-236.

(2) "Über die Methode der Schlierenbeobachtung als mikroskopisches Hülfsmittel, nebst Bermerkungen zur Theorie der Schiefen Beleuchtung" (On the Method of Observing Schlieren as an Aid in Microscopy in Conjunction with Remarks on the Theory of Oblique Illumination), by A. Toepler, J.C. Poggendorff's Annalen der Physik und Chemie, 5th Series, Vol. 127, No. 4, 1 May 1866, pp. 556-580.

(3) "Vibroskopische Beobachtungen über die Schwingungsphasen singender Flammen (der chemischen Harmonica) mit Benutzung des Schlierenapparates" (Vibroscopic Observations on the Phases of Vibration of Singing Flames, i.e., the "Chemical Harmonica," with the Use of the Schlieren Apparatus), by A. Toepler, J.C. Poggendorff's Annalen der Physik und Chemie, Vol. 128, No. 1, 6 June 1866, pp. 126-139.

(4) "Optische Studien nach der Methode der Schlierenbeobachtung" (Optical Studies by the Method of Observing Schlieren), by A. Toepler, J.C. Poggendorff's Annalen der Physik und Chemie, Vol. 131, No. 1, 21 June 1867, pp. 33-35; (continued), Vol. 131, No. 2, pp. 180-215; (concluded), Vol. 134, No. 2, pp. 194-218.

(5) "Über die Momentanbeleuchtung bei Beobachtung der Lichtwellenschlieren" (On Instantaneous Illumination in the Observation of Light-Wave Schlieren), by E. Mach, Poggendorff's Annalen der Physik und Chemie, Vol. 159, (II), No. 10, 9 October 1876, pp. 330-331.

(6) "Optische Untersuchung der Funkenwellen" (Optical Investigation of Waves Produced by Electric Sparks), by E. Mach and G. Gruss, Sitzungsberichte der Kaiserlichen Akademie der Wissenschaften (Mathematisch-Naturwissenschaftliche Klasse), Vol. 78, Part 2-3, No. 2, Vienna, 4 July 1878, pp. 467-480.

(7) Article by Léon Foucault, Recueil des travaux scientifiques, Paris, 1878.

(8) "Über eine neue einfache Art der Schlierenbeobachtung" (On a New Simple Type of Schlieren Observation), by V. Dvorak, G. Wiedemann's Annalen der Physik und Chemie, Vol. 10, No. 3, 15 March 1880, pp. 502-511.

(9) "Über ein Mikrorefraktometer" (On a Microrefractometer), by Prof. Dr. S. Exner, Repertorium der Physik, Vol. 21, 1886, p. 555.

(10) "Über ein Mikrorefraktometer" (On a Microrefractometer), by Prof. Dr. S. Exner, Zeitschrift für Instrumentenkunde, Vol. 6, No. 4, April 1886, pp. 139-141. This is a review by S. Czapsky of the foregoing item.

(11) Article by A. Toepler, Archiv für Artillerie und Ingenieurwesen, 1887, p. 485.

(12) "Photographische Fixierung der durch Projectile in der Luft eingeleiteten Vorgänge" (Photographic Recording of Phenomena Produced in Air by Projectiles), by L. Mach and P. Salcher, Sitzungsberichte der Kaiserlichen Akademie der Wissenschaften (Mathematisch-Naturwissenschaftliche Klasse), Vol. 95, No. 4, Vienna, 21 April 1887, pp. 764-780.

(13) "Über die in Pola und Meppen angestellten ballistisch-photographischen Versuche" (On the Photographic-Ballistic Experiments Devised at Pola and Meppen), by E. Mach and P. Salcher, Sitzungsberichte der Kaiserlichen Akademie der Wissenschaften (Mathematisch-Naturwissenschaftliche Klasse), Vol. 98, Part 2a, No. 1, Vienna, 10 January 1889, pp. 41-50.

(14) "Optische Untersuchung der Luftstrahlen" (Optical Investigation of Streamlines in Air), by E. Mach and P. Salcher, Sitzungsberichte der Kaiserlichen Akademie der Wissenschaften (Mathematisch-Naturwissenschaftliche Klasse), Vol. 98, Part 2a, No. 9, Vienna, 7 November 1889, pp. 1303-1308.

(15) "Weitere ballistisch-photographische Versuche" (Additional Photographic-Ballistic Experiments), by E. Mach and L. Mach, Sitzungsberichte der Kaiserlichen Akademie der Wissenschaften (Mathematisch-Naturwissenschaftliche Klasse), Vol. 98, Part 2a, Vienna, 1889, pp. 1310-1326.

(16) "Über longitudinale fortschreitende Wellen im Glase" (On Longitudinal Propagating Waves in Glass), by E. Mach, Sitzungsberichte der Kaiserlichen Akademie der Wissenschaften (Mathematisch-Naturwissenschaftliche Klasse), Vol. 98, Part 2a, Vienna, 1889, pp. 1327-1332.

(17) "Über die Interferenz der Schallwellen von grosser Excursion" (On the Interference of Sonic Waves of Great Amplitude), by E. Mach and L. Mach, Sitzungsberichte der Kaiserlichen Akademie der Wissenschaften (Mathematisch-Naturwissenschaftliche Klasse), Vol. 98, Part 2a, No. 9, Vienna, 1889, pp. 1333-1336.

(18) "Über die Interferenz der Schallwellen von grosser Excursion" (On the Interference of Sonic Waves of Great Amplitude), by E. Mach and L.

Mach, G. Wiedemann's Annalen der Physik und Chemie, Vol. 41, No. 9, 15 August 1890, pp. 140-143.

(19) "Optische Untersuchung der Luftstrahlen" (Optical Investigation of Air Streamlines), by E. Mach and P. Salcher, G. Wiedemann's Annalen der Physik und Chemie, Vol. 41, No. 9, 15 August 1890, pp. 144-150.

(20) "Darstellung gekrümmter Lichtstrahlen und Verwertung derselben zur Untersuchung von Diffusion und Wärmeleitung" (Production of Refracted Light Rays and their Evaluation for the Investigation of Diffusion and Heat Transmission), by Otto Wiener, G. Wiedemann's Annalen der Physik und Chemie, Vol. 49, No. 5, 15 April 1893, pp. 105-149.

(21) "Über die Sichtbarmachung von Luftstromlinien" (On Making Air Streamlines Visible), by Dr. Ludwig Mach, Vienna, Zeitschrift für Luftschiffahrt und Physik der Atmosphäre, Vol. 15, 1896, pp. 129-139.

(22) "Über die Wirkung des Windes auf schwach gewölbte Flächen" (On the Effect of Wind on Slightly Arched Surfaces), by A. von Obermayer, Zeitschrift für Luftschiffahrt und Physik der Atmosphäre, Vol. 15, 1896, pp. 120-123.

(23) "Weitere Versuche über Projectile" (Additional Experiments on Projectiles), by Dr. Ludwig Mach, Sitzungsberichte der Kaiserlichen Akademie der Wissenschaften (Mathematisch-Naturwissenschaftliche Klasse), Vol. 105, Part 2a, 1896, Vienna, pp. 605-632.

(24) "Übersichtliche Darstellung der optisch-photographischen Untersuchung der durch bewegte Projectile in Luft erregten Vorgänge" (Comprehensive Presentation of the Optical-Photographic Investigations of the Phenomena Produced in Air by Moving Projectiles), by Albert Edl. von Obermayer, Mitteilungen über Gegenstände des Artillerie- und Genie-Wesens, herausgegeben vom K. u. K. Technischen Militär-Comité, Vol. 28, No. 11, Vienna, 1897, pp. 815-835.

(25) "Optische Untersuchung der Luftstrahlen" (Optical Investigation of Streamlines in Air), by Dr. Ludwig Mach, Jena, Sitzungsberichte der Kaiserlichen Akademie der Wissenschaften (Mathematisch-Naturwissenschaftliche Klasse), Vol. 106, Part 2a, No. 10, pp. 1025-1074.

(26) Article by Vielle, Mémoires des Poudres et Salpêtres, Vol. 10, 1899, p. 177.

(27) "Über die Ausströmungserscheinungen permanenter Gase" (On the Phenomena of Flow of Escaping Permanent Gases), by Robert Emden, G. and E. Wiedemann's Annalen der Physik, Vol. 69, No. 9, 14 September 1899, pp. 264-289.

(28) Article by Rieckeherr, Kriegstechnische Zeitschrift für Offiziere aller Waffen, Vol. 3, 1900, pp. 383, 439, 513.

(29) "Photography of Sound-Waves by the 'Schlieren-Methode'," by Prof. R.W. Wood, Philosophical Magazine, 5th Series, Vol. 48, No. 291, August 1899, pp. 218-227.

(30) "Photography of Sound-Waves, and the Kinematographic Demonstration of the Evolutions of Reflected Wave Fronts," by Prof. R.W. Wood, Philosophical Magazine, 5th Series, Vol. 50, No. 302, July 1900, pp. 148-156.

(31) "On the Propagation of Cusped Waves and their Relation to the Primary and Secondary Focal Lines," by Prof. R.W. Wood, Philosophical Magazine, 6th Series, Vol. I (52, old numbering), No. 5, May 1901, pp. 589-593.

(32) "Über die explosionsartige Wirkung moderner Infanteriegeschosse" (On the Explosion-Like Effect of Modern Infantry Projectiles), by C. Cranz and K.R. Koch, Paul Drude's Annalen der Physik, 4th Series, Vol. 3, No. 10, Leipzig, 1900, pp. 247-273.

(33) "Anwendung der elektrischen Momentphotographie auf die Untersuchung von Schusswaffen", (Application of Electrical Instantaneous Photography to the Investigation of Firearms), by C. Cranz, Knapp, Halle, 1900.

(34) "Beiträge zur Theorie der Lichtbahnen und Wellenflächen in heterogenen isotropen Medien" (Contributions to the Theory of the Paths of Light and Wave Planes in Heterogeneous, Isotropic Mediums), by Melchoir Wierz, Dissertation, University of Rostock, 1901.

(35) "The Photography of Sound Waves and Other Disturbances in Air," by H. Stanley Allen, Proceedings of the Royal Philosophical Society of Glasgow, Vol. 33, 1902, pp. 71-80.

(36) "Physical Optics," by R.W. Wood, Macmillan Co., London, 1905, p. 94.

(37) "Labialpfeifen und Lamellentöne" (Labial Organ Pipes and Reed Tones), by R. Wachsmuth, Paul Drude's Annalen der Physik, 4th Series, Vol. 14, No. 8, Leipzig, 1904, pp. 469-505.

(38) "Beobachtungen nach einer neuen optischen Methode" (Observations by a New Optical Method), by A. Toepler, Ostwald's Klassiker der exakten Wissenschaften, No. 157, Leipzig, 1906.

(39) "Beobachtungen nach der Schlierenmethode" (Observations by the Schlieren Method), by A. Toepler, Ostwald's Klassiker der exakten Wissenschaften, No. 158, Leipzig, 1906.

(40) Treatise by R. Straubel, Handbuch der Physik, Winkelmann, Vol. 6, J.A. Barth, Leipzig, 1906, p. 485.

(41) Article by V. Dvorak, Zeitschrift für den physikalischen und chemischen Unterricht, Vol. 21, 1908, p. 17.

(42) Article by Weinhold, Zeitschrift für den physikalischen und chemischen Unterricht, Vol. 21, 1908, p. 281.

(43) "Hydrodynamique Expérimentale: 'Étude cinematographique des remous et des rides produits par la translation d'un obstacle'" (Experimental Hydrodynamics: 'Cinematographic Study of the Vortices and Ripples Produced by Translation of an Obstacle'), by Henri Bénard, Comptes Rendus de l'Académie des Sciences de Paris, Vol. 147, No. 21, 23 November 1908, pp. 970-973.

(44) "Neue, einfache Versuchsanordnung zur bequemen subjektiven Sichtbarmachung von Funkenschallwellen nach der Schlierenmethode" (A New, Simple Experimental Apparatus to Make Sonic Waves Produced by Electric Sparks Visible Conveniently and Subjectively by the Schlieren Method), by Max Toepler, Annalen der Physik, Wien and Planck, Vol. 27, No. 15, 15 December 1908, pp. 1043-1050.

(45) "Zur Kenntnis der Funkenschallwellen elektrischer Oszillationen" (Contribution to Information on the Sonic Waves Produced by Electric Sparks in Electrical Oscillations), by Max Toepler, Annalen der Physik, Wien and Planck, Vol. 27, No. 15, 15 December 1908, pp. 1051-1058.

(46) "Aérodynamique: 'Étude photographique du courant d'air produit par le mouvement d'une hélice'" (Aerodynamics: 'Photographic Study of the Slipstream Produced by a Rotating Propeller in Air'), by A. Tanakadaté, Comptes Rendus de l'Académie des Sciences de Paris, Vol. 151, No. 3, 18 July 1910, pp. 211-223.

(47) "La photographie du vent" (Photographing Air Currents), by Capt. A. Lafay, La Technique Aéronautique, Vol. 3, First Semester, Paris, 1900, pp. 169-177.

(48) "Étude photographique du champ aérodynamique" (Photographic Study of the Aerodynamic Field), by Capt. A. Lafay, La Technique Aéronautique, Vol. 4, Second Semester, Paris, 1911, pp. 91-98.

(49) "Physique: Sur l'utilisation du procédé d'exploration à l'acétylène pour la mesure de la vitesse du vent et l'étude du champ aérodynamique" (On the Use of the Acetylene Method of Investigation for the Measurement of the Velocity of the Wind and for the Study of the Aerodynamic

Field), by A. Lafay, Comptes Rendus de l'Académie des Sciences de Paris, Vol. 152 (I), No. 11, March 13, 1911, pp. 694-696.

(50) Article by C. Cranz and P.A. Günther, Zeitschrift für das gesamte Schiess- und Sprengstoffwesen, Vol. 7, 1912, p. 317.

(51) "Photographische Aufnahme von sehr rasch verlaufenden Vorgängen, insbesondere von Schussvorgängen, mittels Vorderbeleuchtung durch das Licht elektrischer Funken" (Photography of Very High-Speed Phenomena, Especially Ballistic Phenomena, by Frontal Illumination with Electric Sparks), by C. Cranz, P.A. Günther, and F. Külp, Zeitschrift für das gesamte Schiess- und Sprengstoffwesen, Vol. 9, No. 4, 15 February 1914, pp. 61-64, plus 4 excellent plates.

(52) "Die Ausströmung von Gasen bei hohen Anfangsdrucken, I. Teil" (The Flow of Escaping Gases at High Initial Pressures, Part I), by C. Cranz and B. Glatzel, Annalen der Physik, Wien and Planck, Vol. 43, No. 8, 16 April 1914, pp. 1186-1204.

(53) "Beiträge zur Waffenuntersuchung" (Contributions to the Investigation of Weapons), by C. Cranz and F. Külp, Artilleristische Monatshefte, No. 88, April 1914, pp. 251-262, plus 7 plates.

(54) "Free and Forced Convection from Heated Cylinders in Air," by Bidhubhusan Ray, Proceedings of the Indian Association for the Cultivation of Science, Vol. VI, Parts I and II, Calcutta, 1920, pp. 95-107.

(55) "An Optical Study of Free and Forced Convection from Thin Heated Wires in Air," by Satish Chandra Pramanik, Proceedings of the Indian Association for the Cultivation of Science, Vol. VII, Parts III and IV, Calcutta, 1922, pp. 115-123.

(56) Article by C. Cranz and E. Bames, Zeitschrift für angewandte Chemie, Vol. 36, 1923, p. 76.

(57) "Free Convection of Heat in Liquids," by Roy A. Nelson, The Physical Review, a Journal of Experimental and Theoretical Physics, Vol. 23, No. 1, January 1924, pp. 94-103.

(58) "Kinematographic Study on Aeronautics," Provisional Report, by Kwan-ichi Terazawa, Kichisuke Yamazaki, and Yuzo Akishino, Reports of the Aeronautical Research Institute, Tokyo Imperial University, Vol. 1, No. 8, September 1924, pp. 213-223, and 4 full-page photographic plates. (The No. 8 refers to Report No. 8.)

(59) "The Observation of Cataphoresis in Colourless Sols: 1. The Charge on Rubber in Benzene," by R.H. Humphry and R.S. Jane, Transactions of the Faraday Society, Vol. 22, Part 6, No. 70, November 1926, pp. 420-426.

(60) "The Pressure Wave Sent out by an Explosive. Part I," by W. Payman and H. Robinson, Mines Department, Safety in Mines Research Board, Paper 18, London, 1926, 60 pp; ibid, Paper 29.

(61) "Lehrbuch der Ballistik" (Textbook of Ballistics), by C. Cranz, 2nd ed., Vol. 3, Julius Springer, Berlin, 1927, pp. 259 and 264.

(62) "Handbuch der physikalischen und technischen Mechanik" (Manual of Physical and Technical Mechanics), by F. Auerbach and W. Hort, Vol. 5, J.A. Barth, Leipzig, 1928, p. 486.

(63) "Kinematographie auf ruhendem Film und mit extrem hoher Bildfrequenz" (Cinematography on Stationary film at Extremely High Image Frequency), by C. Cranz and H. Schardin, Zeitschrift für Physik, Vol. 56, 1929, pp. 147-183.

(64) "Lehrbuch der praktischen Physik" (Textbook of Practical Physics), by F. Kohlrausch, 6th ed., B. Teubner, Leipzig and Berlin, 1920, p. 304.

(65) "Schlieren-Kinematographie" (Schlieren Cinematography), by Dr. Paul Schrott, Die Kinotechnik, Vol. 12, No. 2, 1930, pp. 40-46.

(66) "Schlierenaufnahmen des Temperaturfeldes in der Nähe wärmeabgebender Körper" (Schlieren Photographs of the Temperature Field in the Vicinity of Bodies Emitting Heat), by E. Schmidt, Zeitschrift des Vereines Deutscher Ingenieure, Vol. 74 (2), No. 43, 25 October 1930, pp. 1487-1488.

(67) "Mehrfachfunkenaufnahmen von Explosionsvorgängen nach der Toeplerschen Schlierenmethode" (Multiple Spark Photography of Explosive Phenomena by Toepler's Schlieren Method), by Dr-Ing. Werner Linder, Forschungsarbeiten auf dem Gebiete des Ingenieurwesens, No. 326, VDI-Verlag, Berlin, 1930, 18 pp.; TMB Translation 121.

(68) "Électricité et Optique: 'Les ondes stationnaires ultrasonores rendues visibles dans les gaz par la méthode des stries'" (Electricity and Optics: 'Stationary Supersonic Waves Made Visible in Gases by the Schlieren Method'), by Edgar-Pierre Tawil, Comptes Rendus de l'Académie des Sciences de Paris, Vol. 191, No. 2, 16 July 1930, pp. 92-95.

(69) "Méthode d'observation d'ondes sonores non stationnaires" (Method of Observing Nonstationary Sonic Waves), by Edgar-Pierre Tawil,

Comptes Rendus de l'Académie des Sciences de Paris, Vol. 191, No. 21, 24 November 1930, pp. 998-1000.

(70) "Optische Homogenitätsprüfung von Filmfolien" (Optical Test to Determine the Homogeneity of Photographic Film), by Dr. K. Kieser Beul, Die Photographische Industrie, Vol. 28, No. 27, 2 July 1930, pp. 729-730; same item: Zeitschrift für angewandte Chemie, Vol. 43, No. 25, 21 June 1930, p. 587.

(71) Treatise by O. Tietjens, Handbuch der Experimentalphysik, W. Wien and F. Harms, Vol. 1, Leipzig, 1931, p. 695.

(72) "The Photography of Waves and Vortices Produced by the Discharge of an Explosive," by D.B. Gawthrop, W.C.F. Shepherd, and G. St. J. Perrott, Journal of the Franklin Institute, Vol. 211, No. 1, January 1931, pp. 67-86.

(73) "Explosion Waves and Shock Waves. Part I - The Wave-Speed Camera and its Application to the Photography of Bullets in Flight," by William Payman, D.Sc., Ph.D., and Donald Whitley Woodhead, M.Sc., Proceedings of the Royal Society, Mathematical and Physical Sciences, Series A, Vol. 132, No. A819, 2 July 1931, pp. 200-213.

(74) "The Phenomenon of Slip in Plastic Materials," by A. Nadai, Proceedings of the American Society for Testing Materials, Part II, Technical Papers, Vol. 31, December 1931, pp. 11-46.

(75) "Experimentelle Untersuchung zur Schneidetonbildung" (Experimental Investigations of the Formation of Tones by Movement of Air Past a Knife Edge), by Heinz Klug, M. Planck's Annalen der Physik, 5th Series, Vol. 11, (Vol. 403 of the complete series), No. 1, 2 September 1931, pp. 53-72.

(76) "Propagation Tests and the Photography of the Disturbance Sent Out by the Explosion of Commercial Electric Detonators," by D.B. Gawthrop, Journal of the Franklin Institute, Vol. 214, No. 6, December 1932, pp. 647-664.

(77) Article by W. Bucerius, Betriebsführung städtischer Werke, Vol. 11, 1932, p. 33.

(78) "Schlierenaufnahmen des Temperaturefeldes" (Schlieren Photographs of the Temperature Field), by Schmidt, Forschung auf dem Gebiete des Ingenieurwesens, Vol. 3, 1932, p. 181.

(79) "Schornsteinfeger und Technik" (Chimney-Sweep and Technology), by W. Bucerius, Berlin, 1932, pp. 57 and 65.

(80) Article by H. Schardin, Heizung und Lüftung, 1932.

(81) "Die Grenzen der Schneidgeschwindigkeit beim Brennschneiden" (The Limits of Cutting Speed in Cutting with the Oxyacetylene Torch), by Hermann Malz, Dissertation of the University of Berlin, 1932.

(82) Article by H. Malz and Conrady, Autogene Metallbearbeitung, Halle a.S., Vol. 25, 1932, p. 117.

(83) "Ignition of Fire Damp by Explosives," by W.C.F. Shepherd, U.S. Bureau of Mines Bulletin 354, 1932.

(84) "Das National Physical Laboratory" (The National Physical Laboratory), by S. Erk, Zeitschrift des Vereines Deutscher Ingenieure, Vol. 77 (2), No. 41, 14 October 1933, pp. 1119-1120.

(85) "The Formation of Localized Slip Layers in Metals," by C.W. MacGregor, Metals and Alloys: The Magazine of Metallurgical Engineering, Vol. 4, No. 2, February 1933, pp. 19-22

(86) "Scientific Instruments and Apparatus: The Physical Society's Annual Exhibition" (Anonymous), World Power, The Monthly Journal of the British Electrical and Allied Manufacturer's Association, Vol. 19, No. 60, February 1933, pp. 75-79.

(87) "Improvements in the Schlieren Method," by H.G. Taylor, M.Sc., (Eng) and J.M. Waldram, B.Sc., Journal of Scientific Instruments, Vol. 10, No. 12, December 1933, pp. 378-389.

(88) "Improvements in the Schlieren Method," by A.G.C. Gwyer, Journal of Scientific Instruments, Vol. 11, No. 1, January 1934, p. 31. Correspondence: Note to article by Taylor and Waldram suggesting use of brushed aluminum sheets manufactured by Gwyer's firm in 2-foot sizes instead of aluminum plates striated by hand with emery cloth.

(89) "Experimentelle Untersuchung Über die Streifenbildung bei Tankentwicklung" (Experimental Investigation of Streak Formation Produced in the Film Developing Tank), by F. Luft, Photo-Woche, Vol. 24, No. 2, 17 October 1933; reviewed: Die Kinotechnik, Vol. 16, No. 2, 20 January 1934, pp. 27-28.

(90) "Improvements in the Schlieren Method of Photography," by H.C.H. Townend, D.Sc., Aerodynamics Department, the National Physical Laboratory, Teddington, Journal of Scientific Instruments, Vol. 11, No. 6, June 1934, pp. 184-187.

PREC-2466-7-10-47-100